# Supporting Information

## Salen complexes of Zirconium and Hafnium: Synthesis, structural characterization and polymerization studies

Mrinmay Mandal,‡[a] Venkatachalam Ramkumar[b] and Debashis Chakraborty*[b]

[a]Department of Chemistry, Indian Institute of Technology Patna, Bihta 801103, Bihar, India. [b]Department of Chemistry, Indian Institute of Technology Madras, Chennai-600 036, Tamil Nadu, India. Fax: +044-22574202; Tel: +044-22574223; E-mail: dchakraborty@iitm.ac.in, debashis.iitp@gmail.com.

‡Current address: School of Chemical and Biomolecular Engineering, Georgia Institute of Technology, Atlanta, GA 30332-0100, United States.

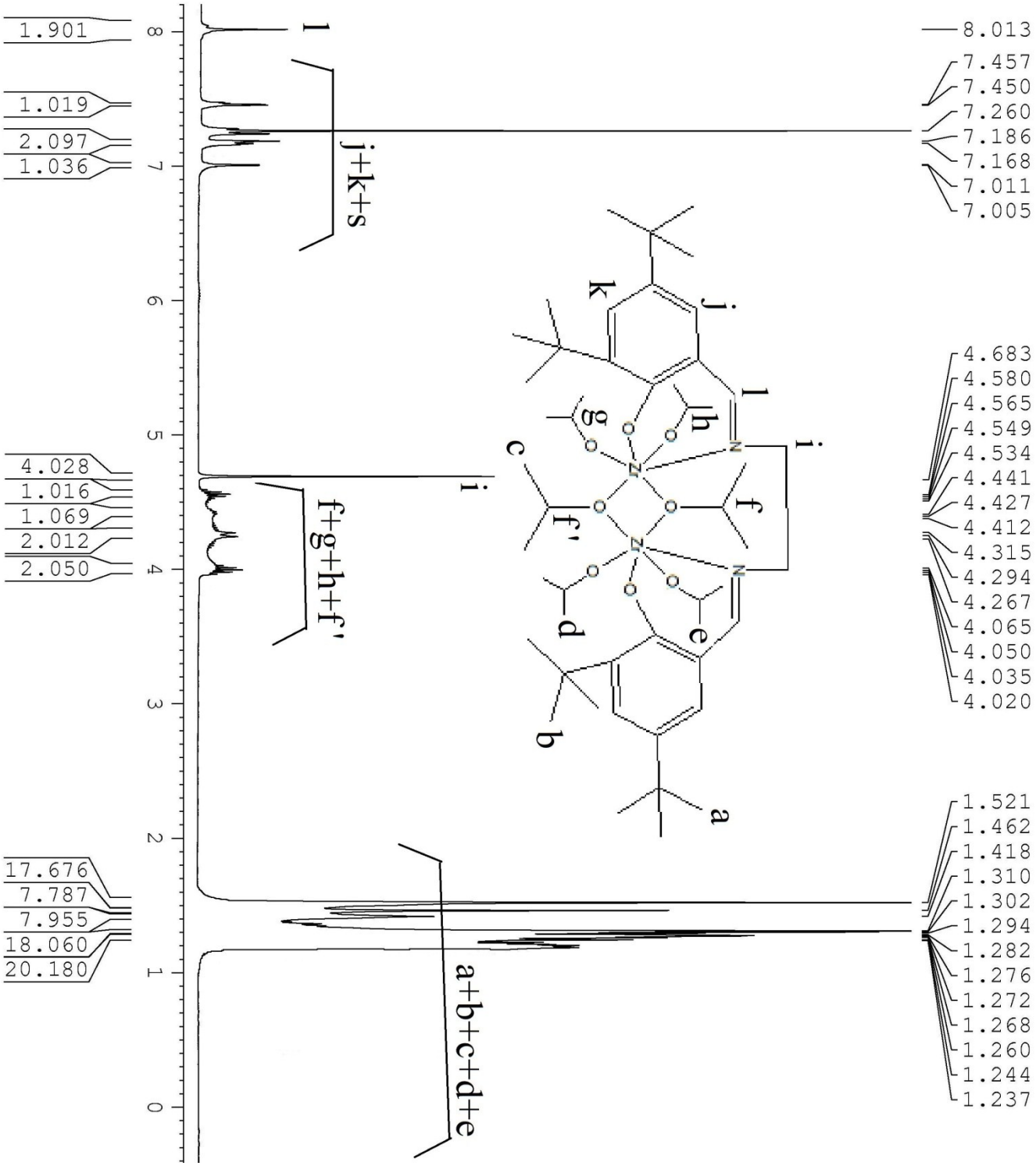
8.013
7.457
7.450
7.260
7.186
7.168
7.011
7.005
4.683
4.580
4.565
4.549
4.534
4.441
4.427
4.412
4.315
4.294
4.267
4.065
4.050
4.035
4.020
1.521
1.462
1.418
1.310
1.302
1.294
1.282
1.276
1.272
1.268
1.260
1.244
1.237
1.901
1.019
2.097
1.036
4.028
1.016
1.069
2.012
2.050
17.676
7.787
7.955
18.060
20.180
l
j+k+s
i
f+g+h+f'
a+b+c+d+e
a
b
c
d
e
f
f'
g
h
i
j
k
l

**Fig. S1** $^1$H NMR (400 MHz, $CDCl_3$) of Compound **1**

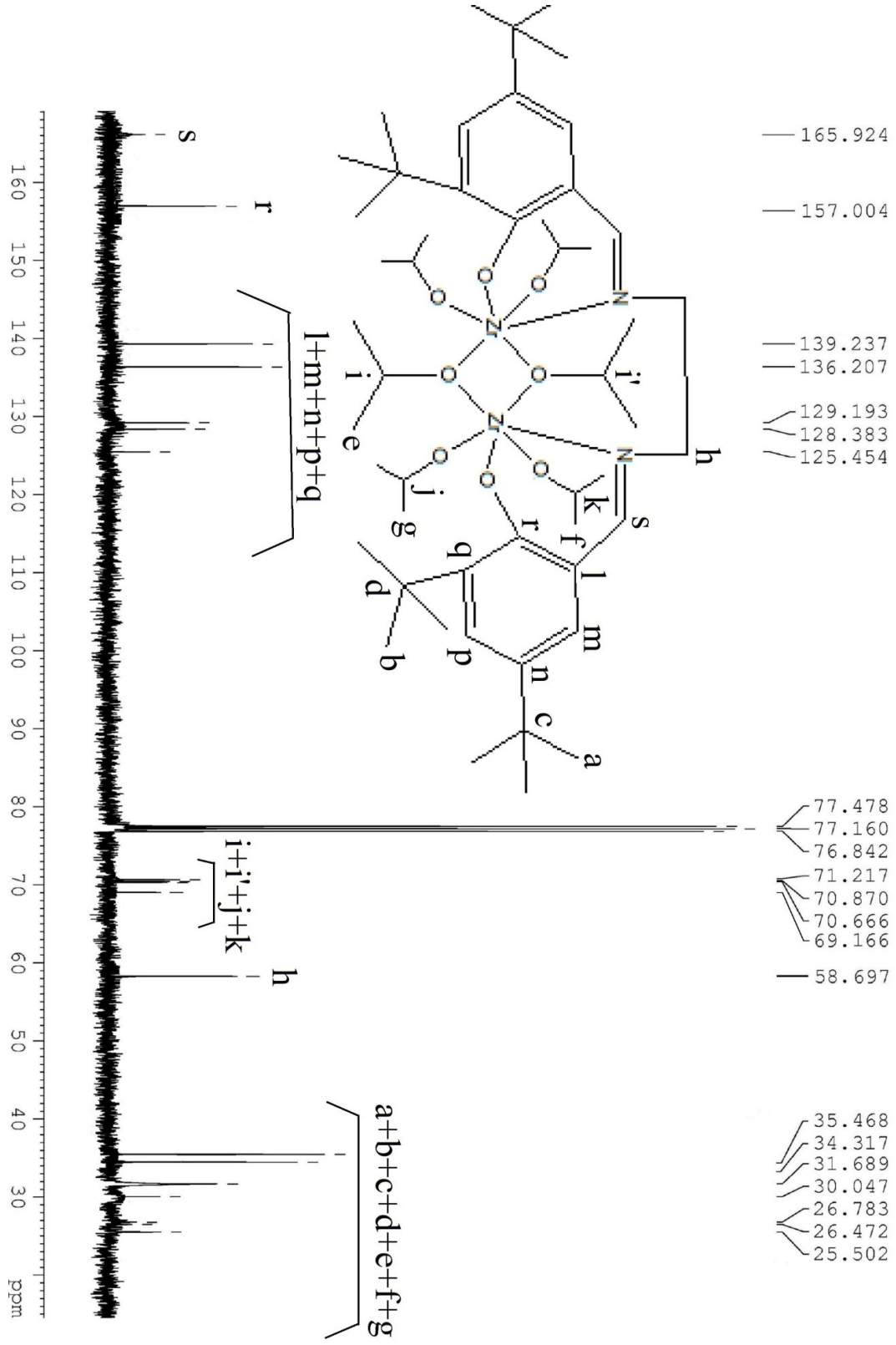

**Fig. S2** $^{13}C$ NMR (100 MHz, $CDCl_3$) of Compound **1**

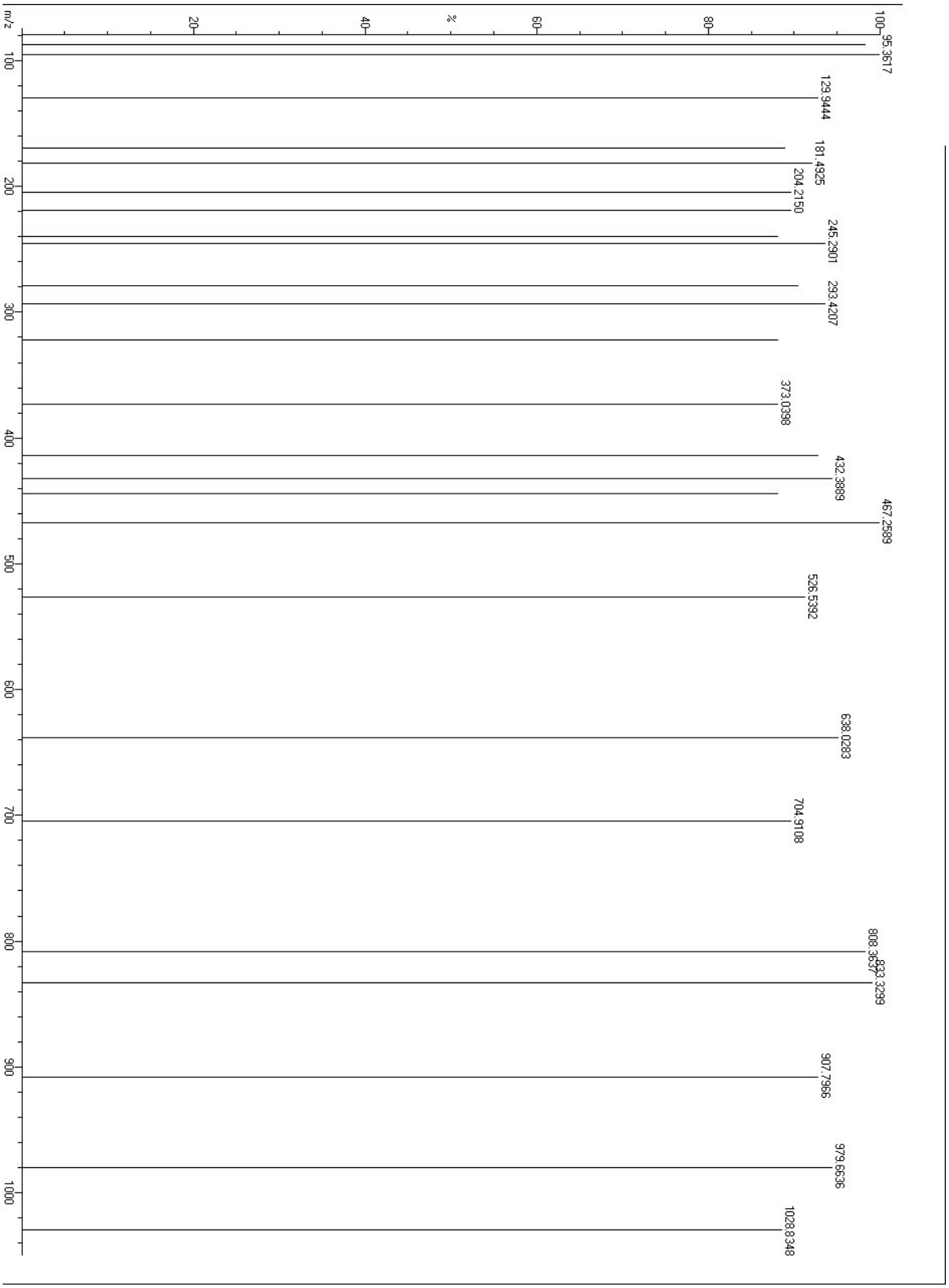

**Fig. S3** ESI-Mass spectrum of Compound **1**

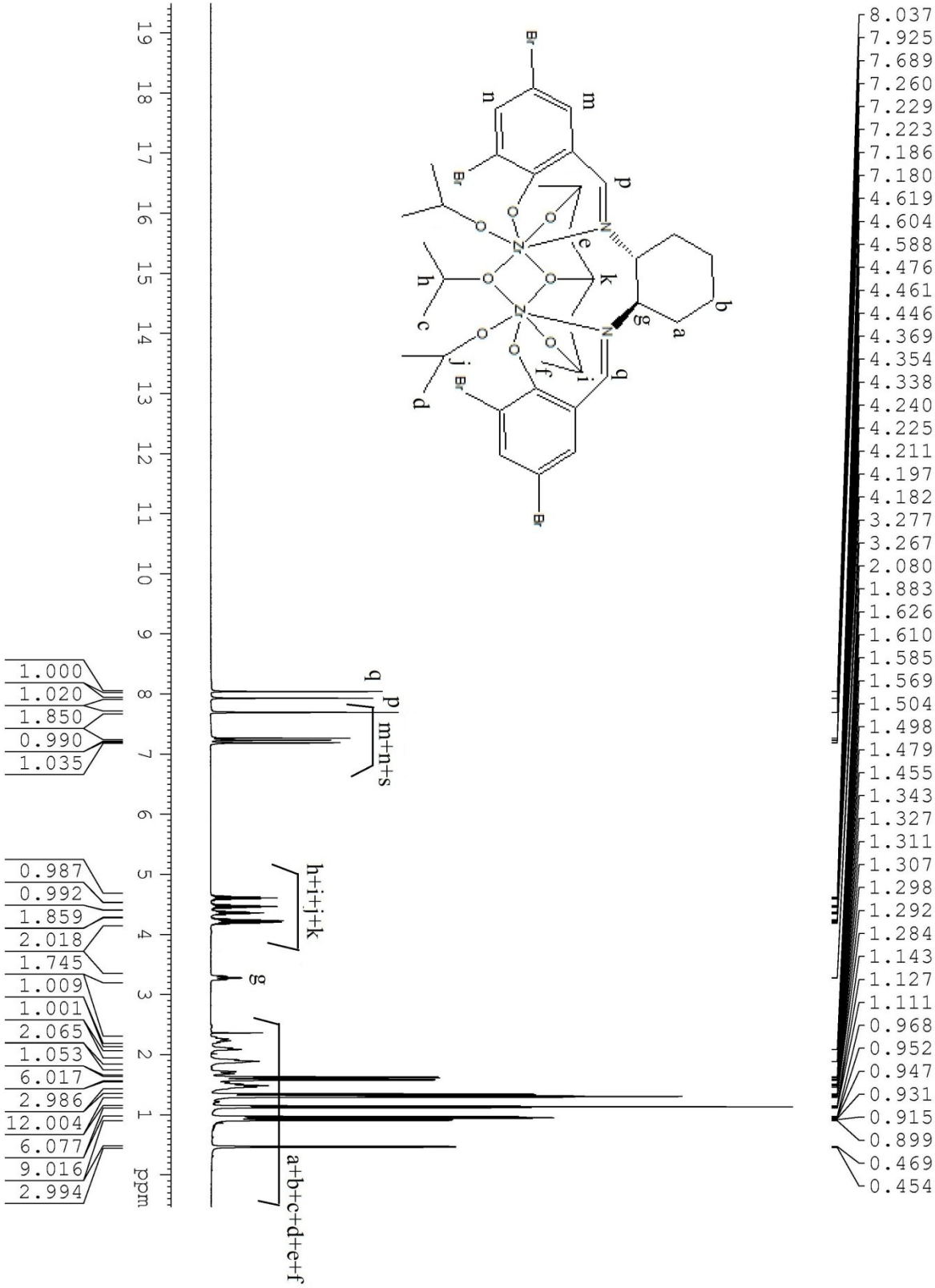

**Fig. S4** $^{1}H$ NMR (400 MHz, $CDCl_3$) of Compound **2**

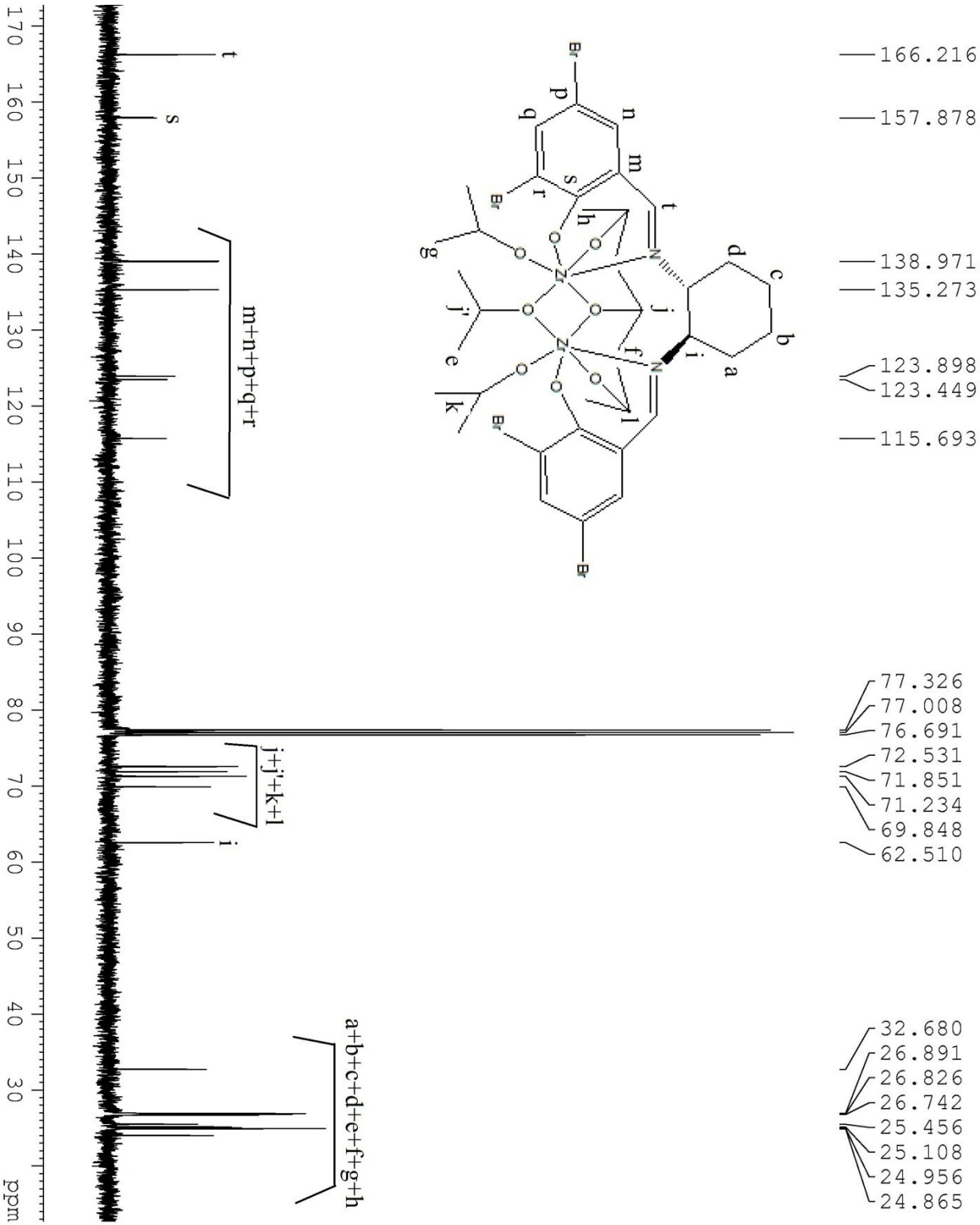


**Fig. S5** $^{13}C$ NMR (100 MHz, $CDCl_3$) of Compound **2**

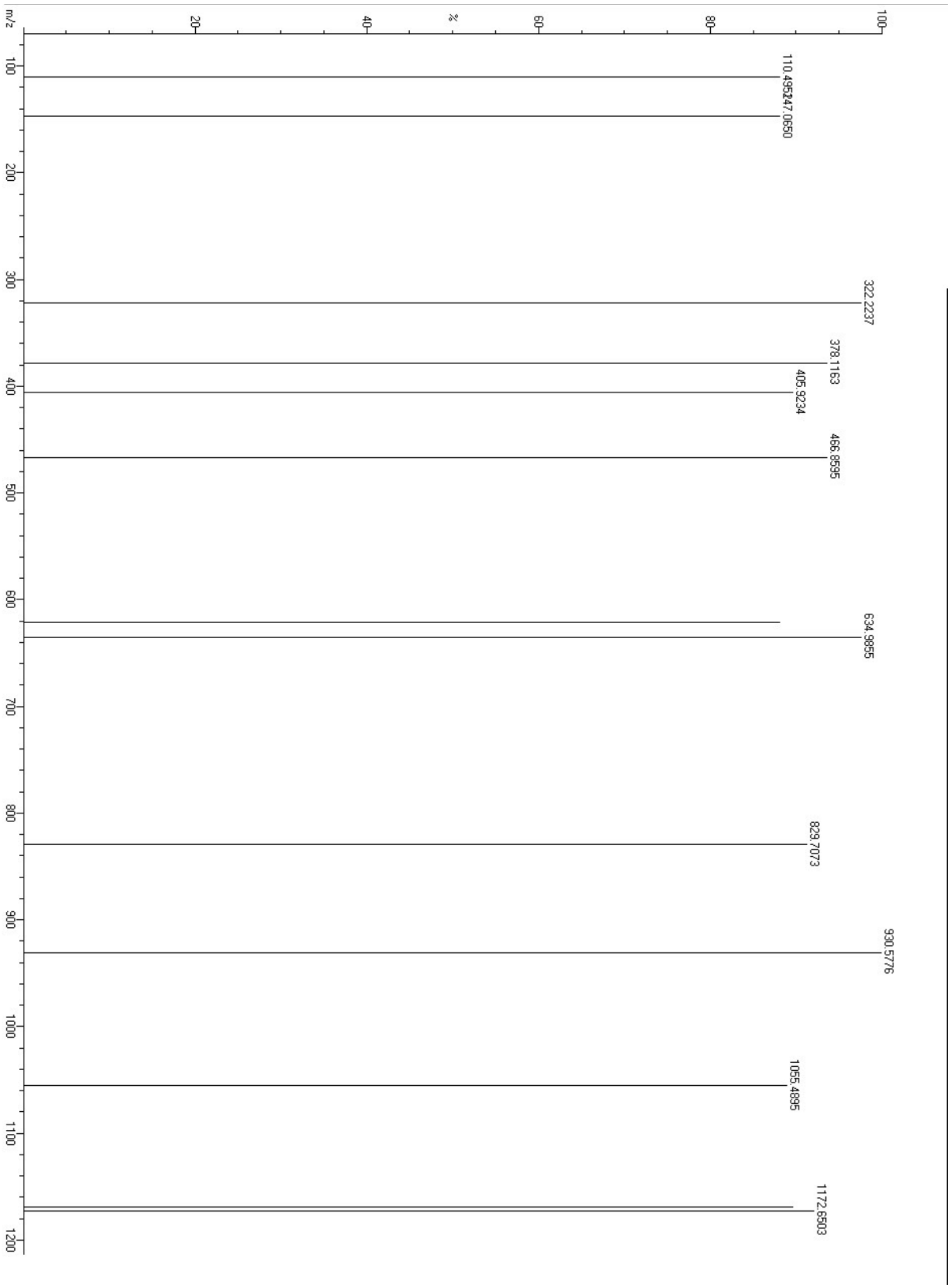


**Fig. S6** ESI-Mass spectrum of Compound **2**

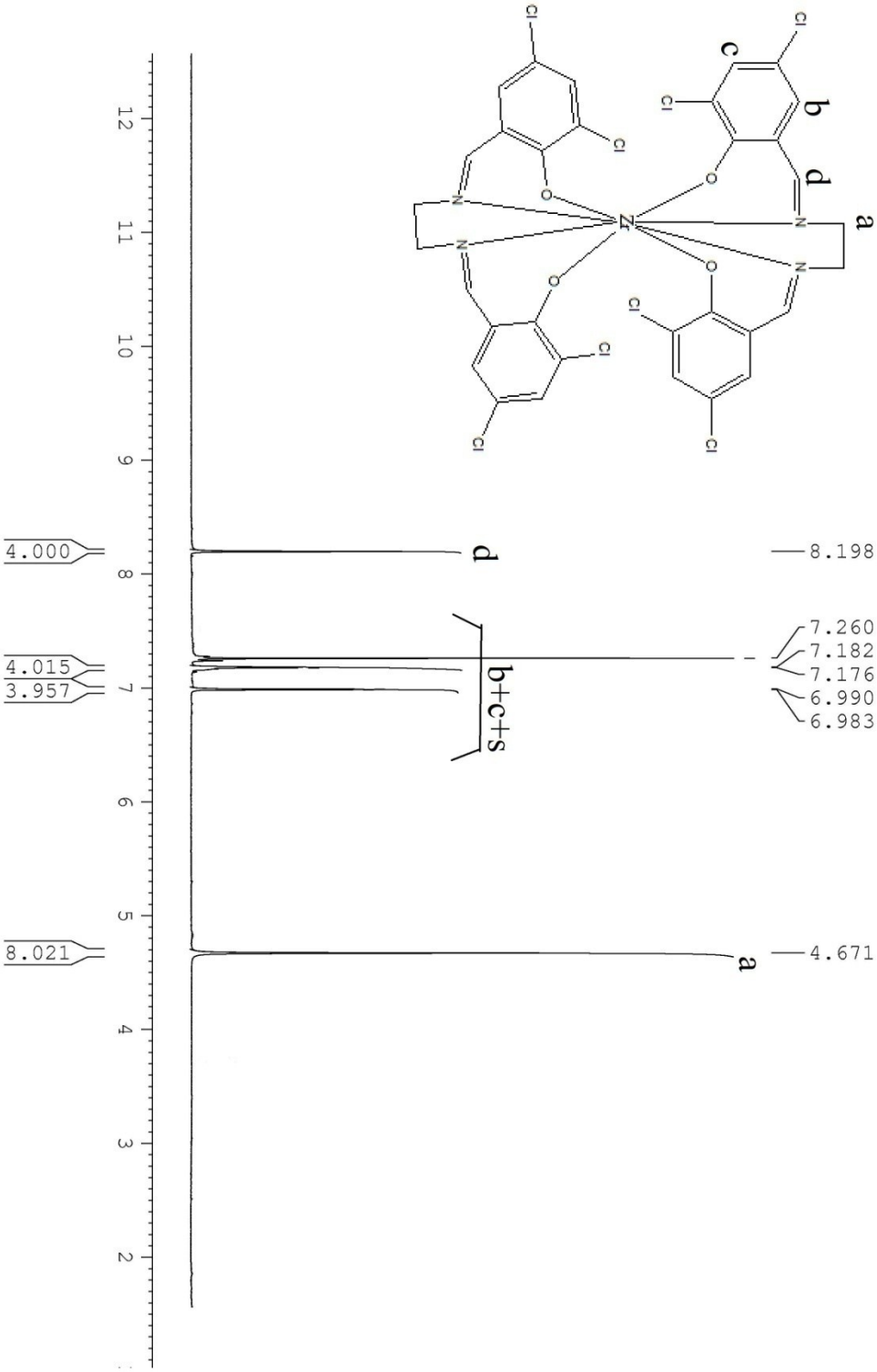


**Fig. S7** $^{1}$H NMR (400 MHz, $CDCl_3$) of Compound **3**

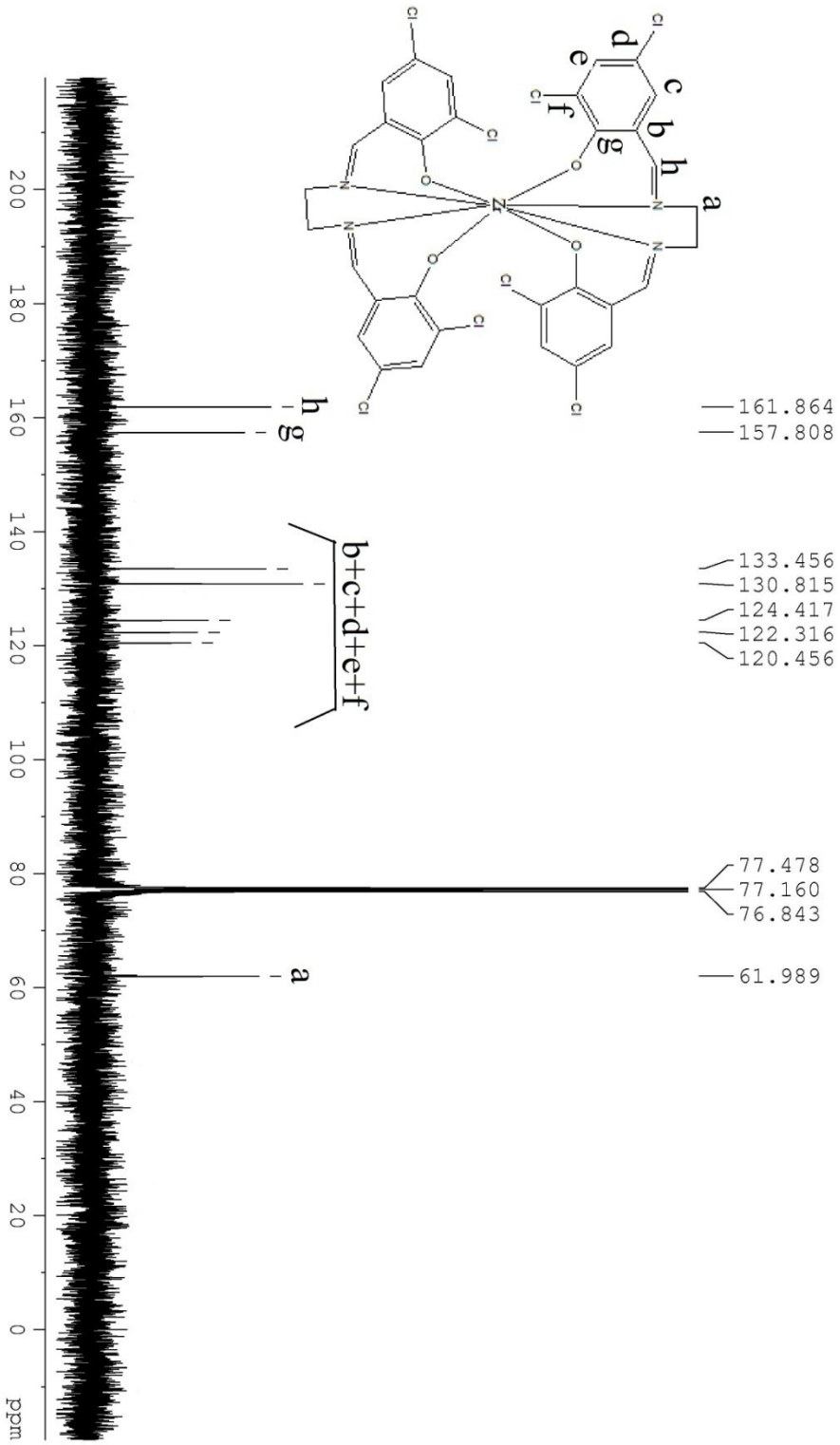


**Fig. S8** $^{13}C$ NMR (100 MHz, $CDCl_3$) of Compound **3**

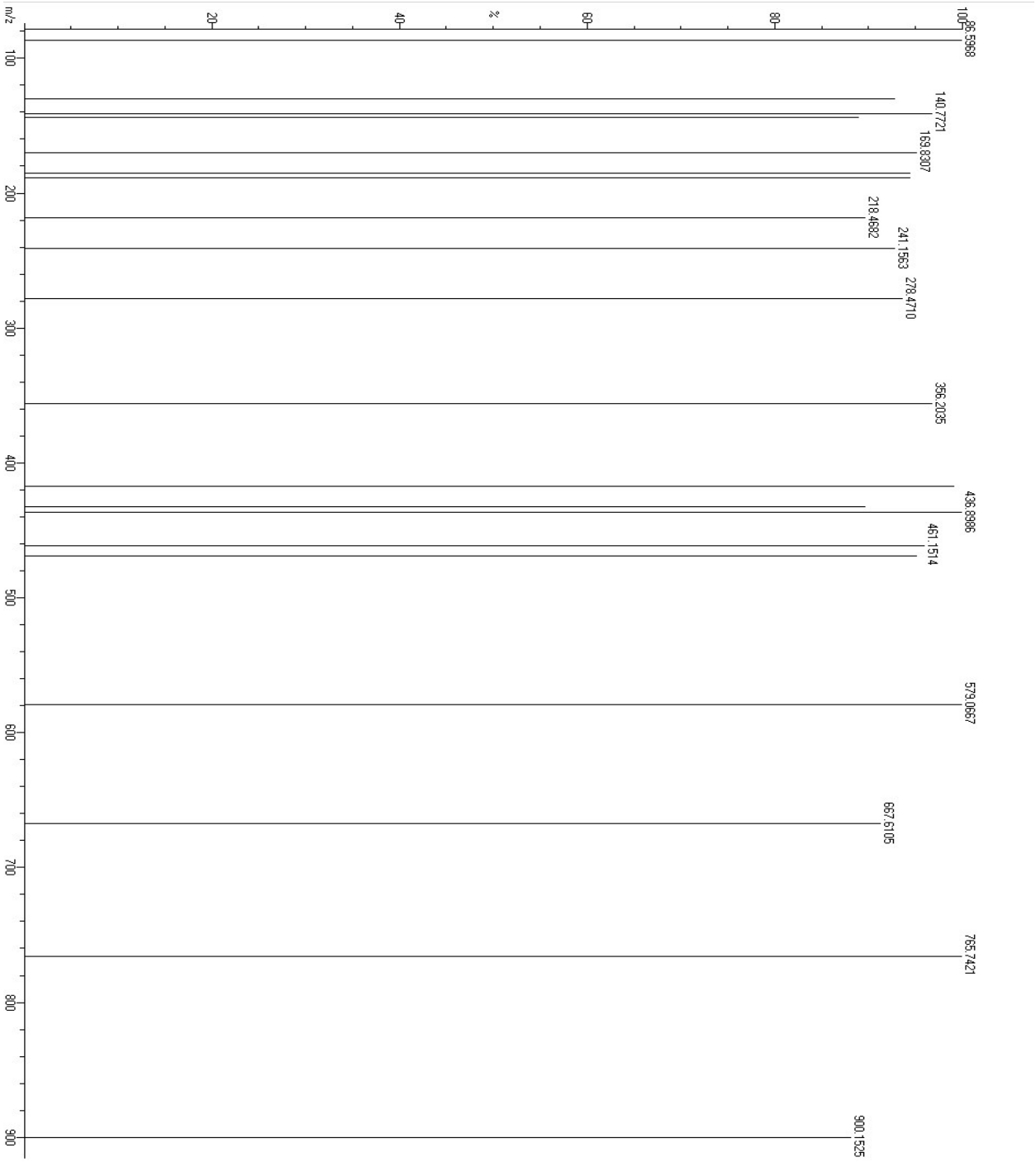


**Fig. S9** ESI-Mass spectrum of Compound **3**

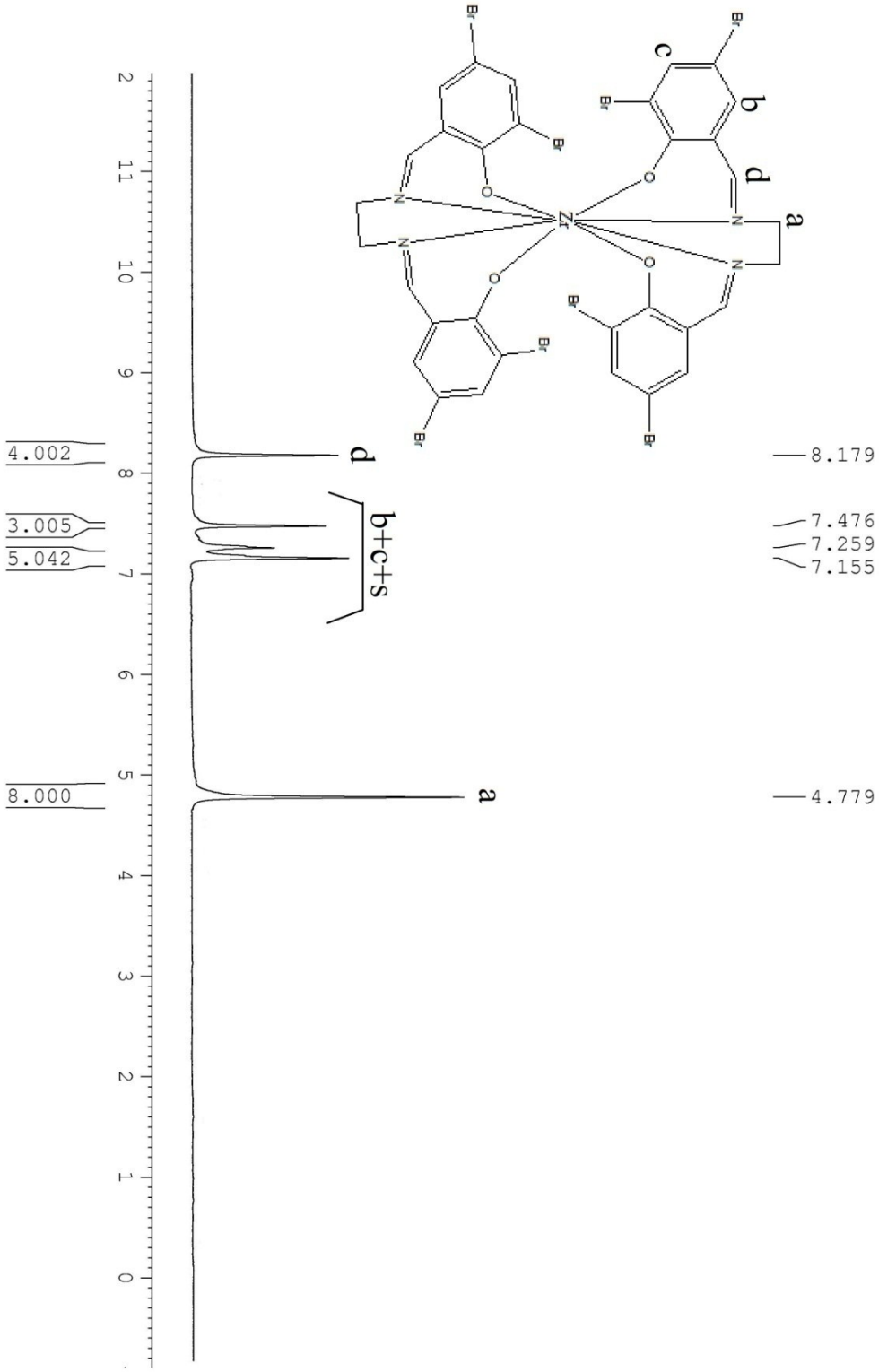


**Fig. S10** $^{1}$H NMR (400 MHz, $CDCl_3$) of Compound **4**

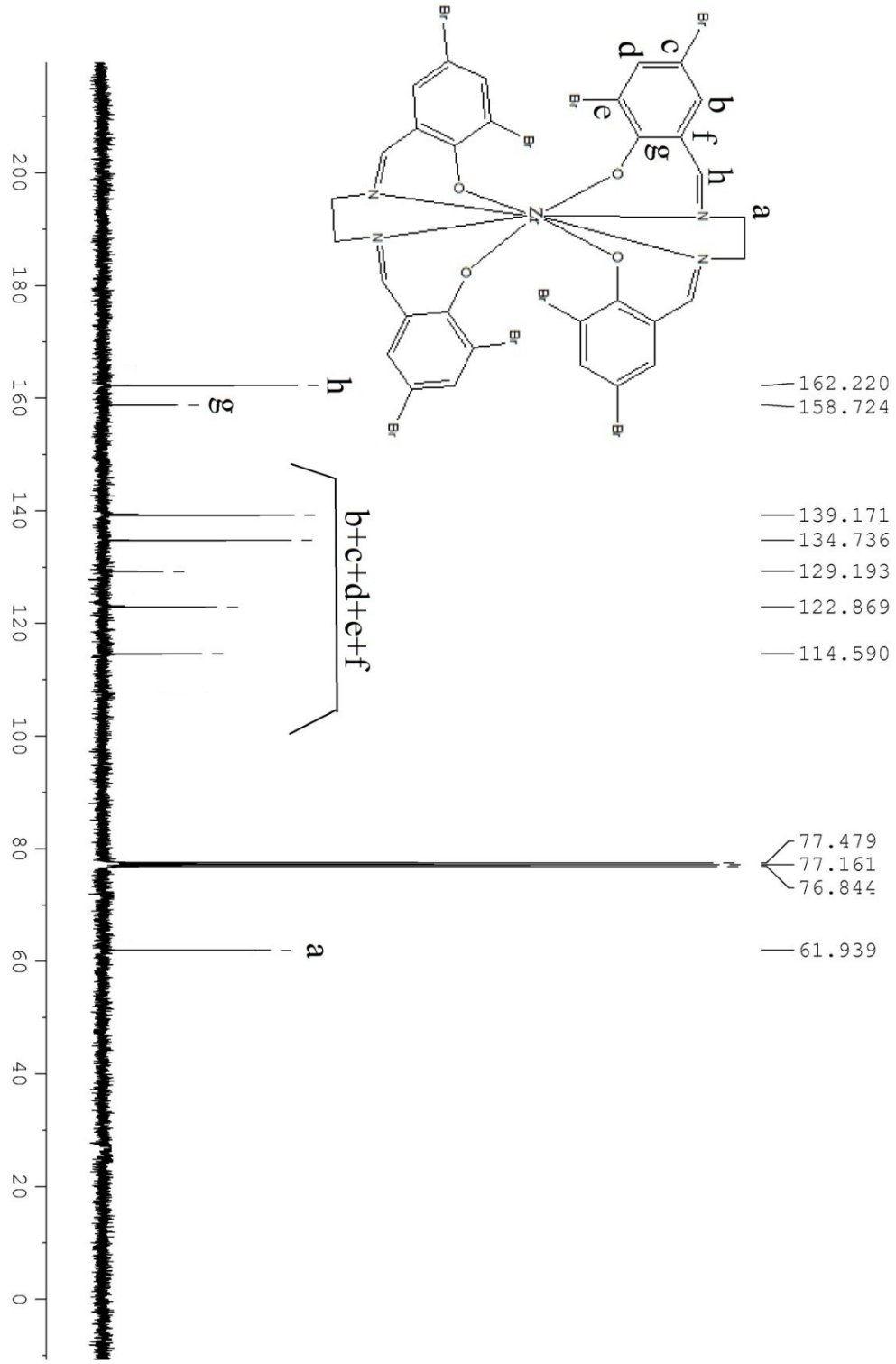


**Fig. S11** $^{13}C$ NMR (100 MHz, $CDCl_3$) of Compound **4**

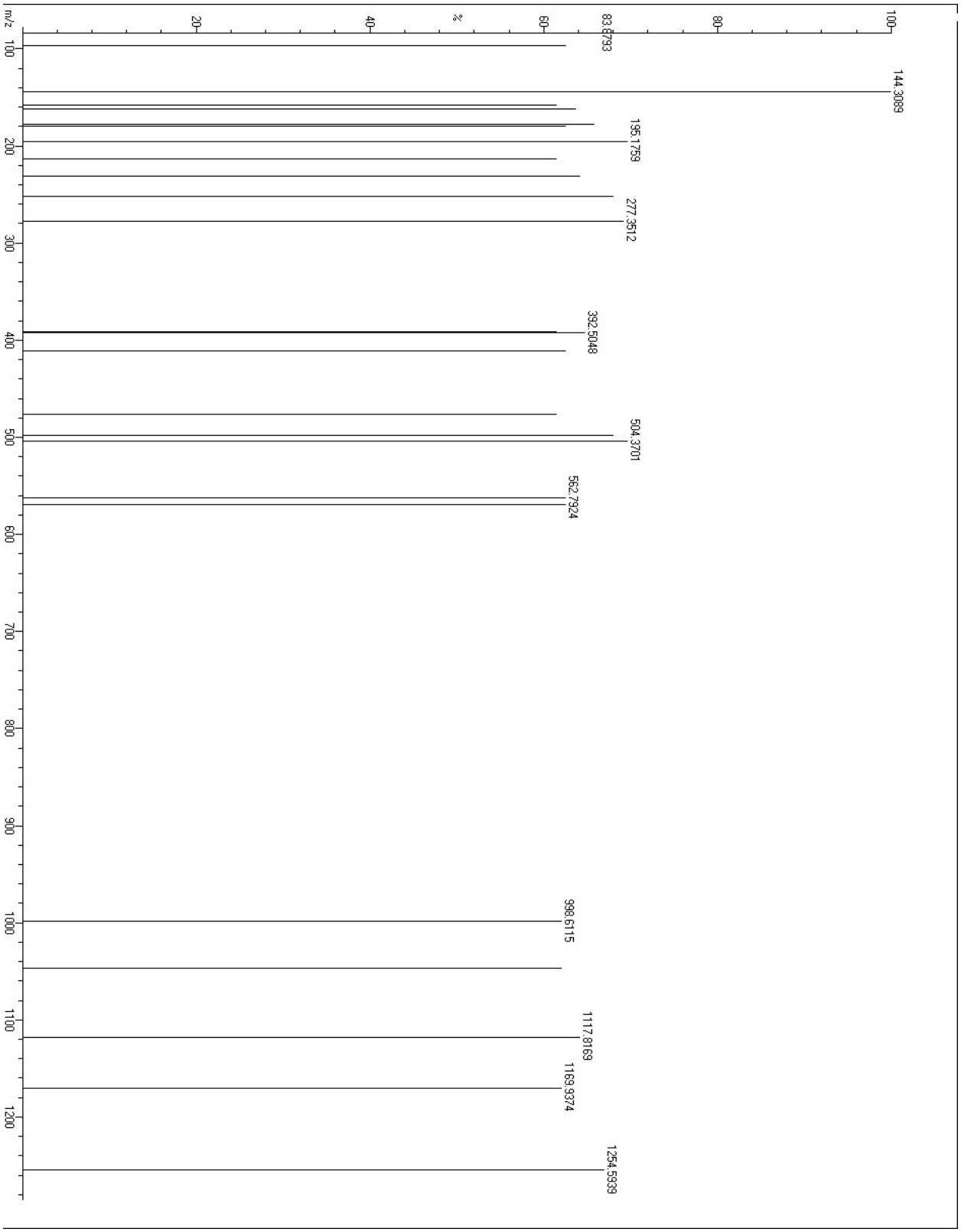


**Fig. S12** ESI-Mass spectrum of Compound **4**

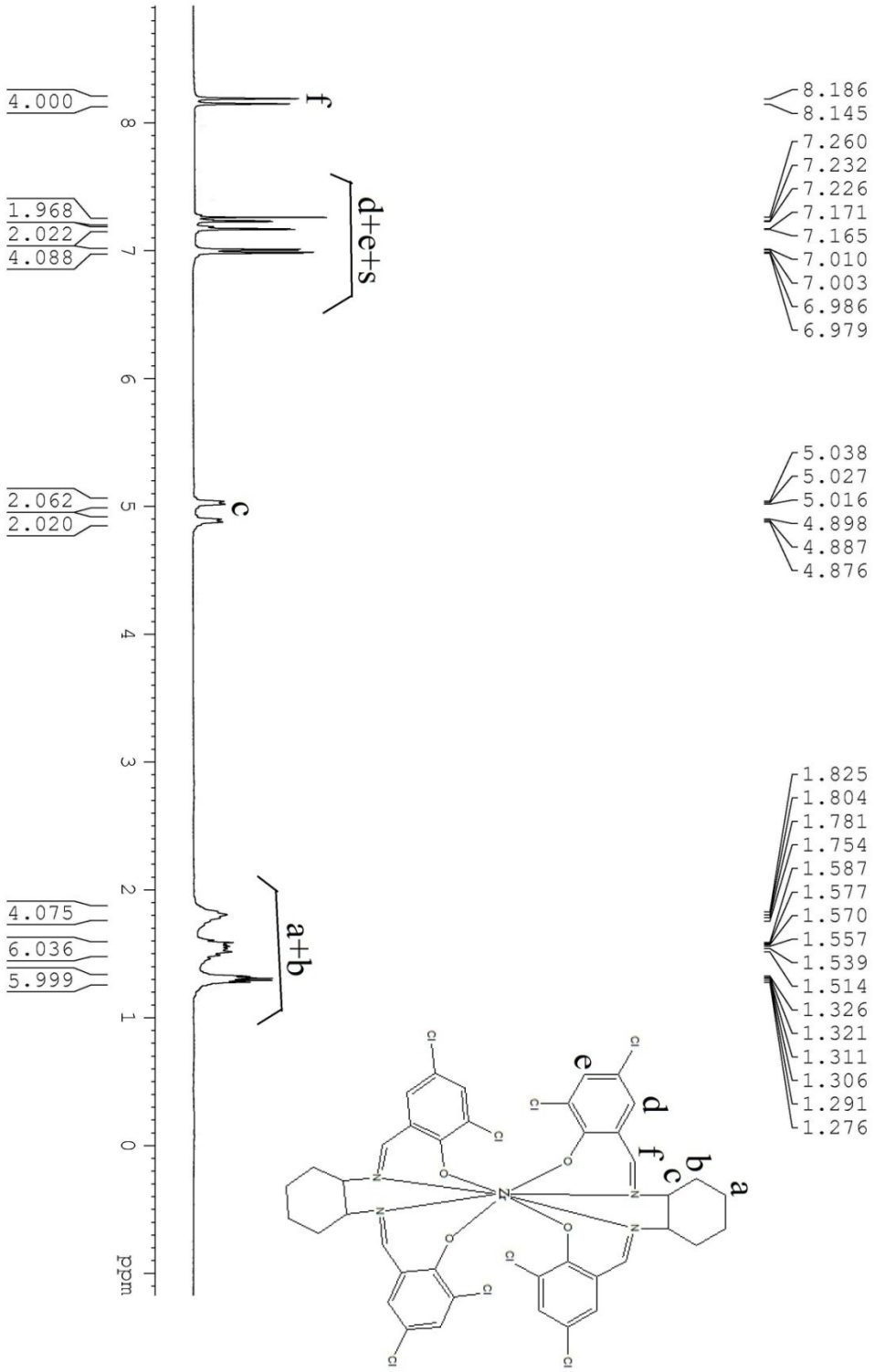


**Fig. S13** $^{1}$H NMR (400 MHz, $CDCl_3$) of Compound **5**

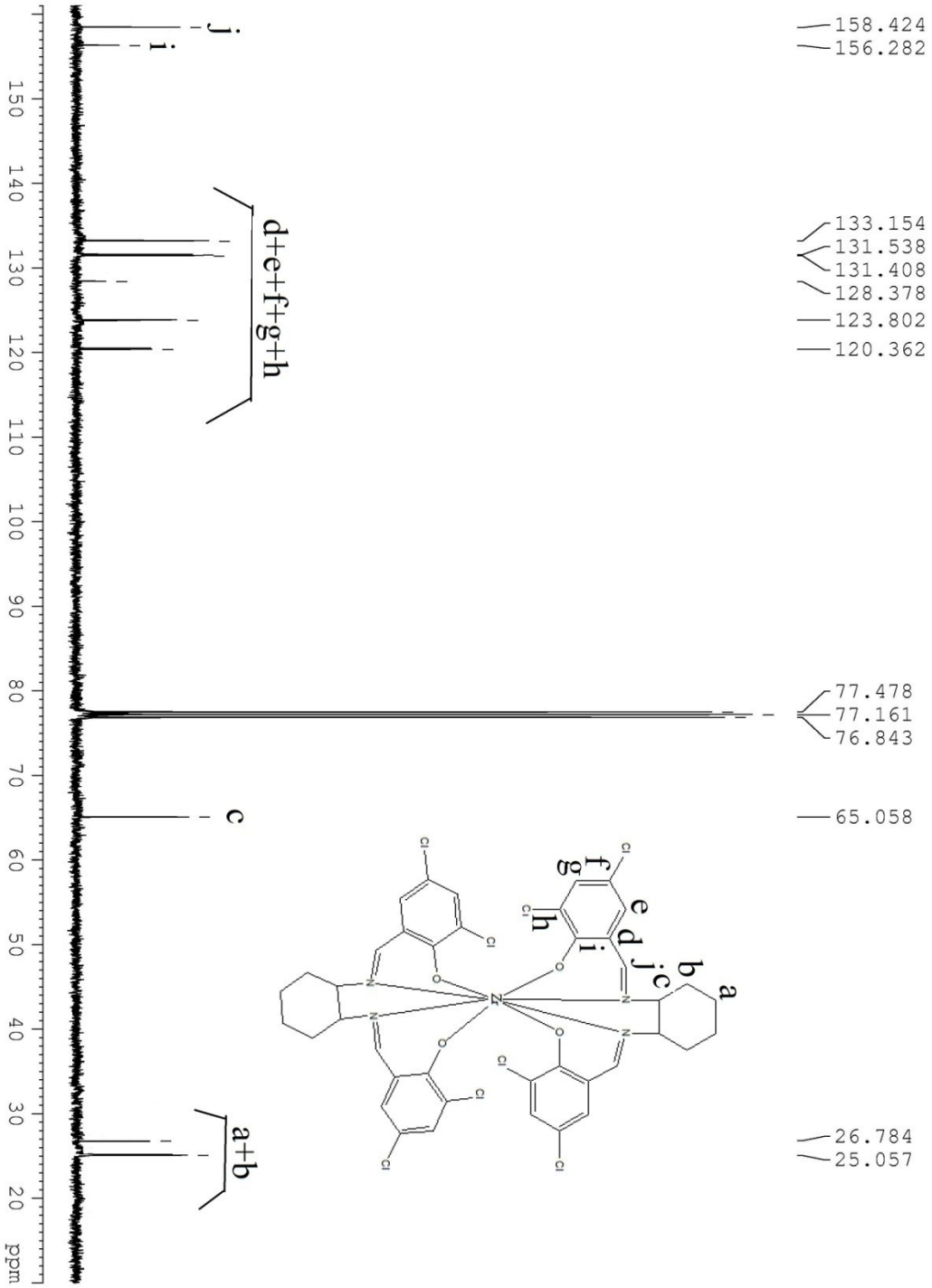


**Fig. S14** $^{13}C$ NMR (100 MHz, $CDCl_3$) of Compound **5**

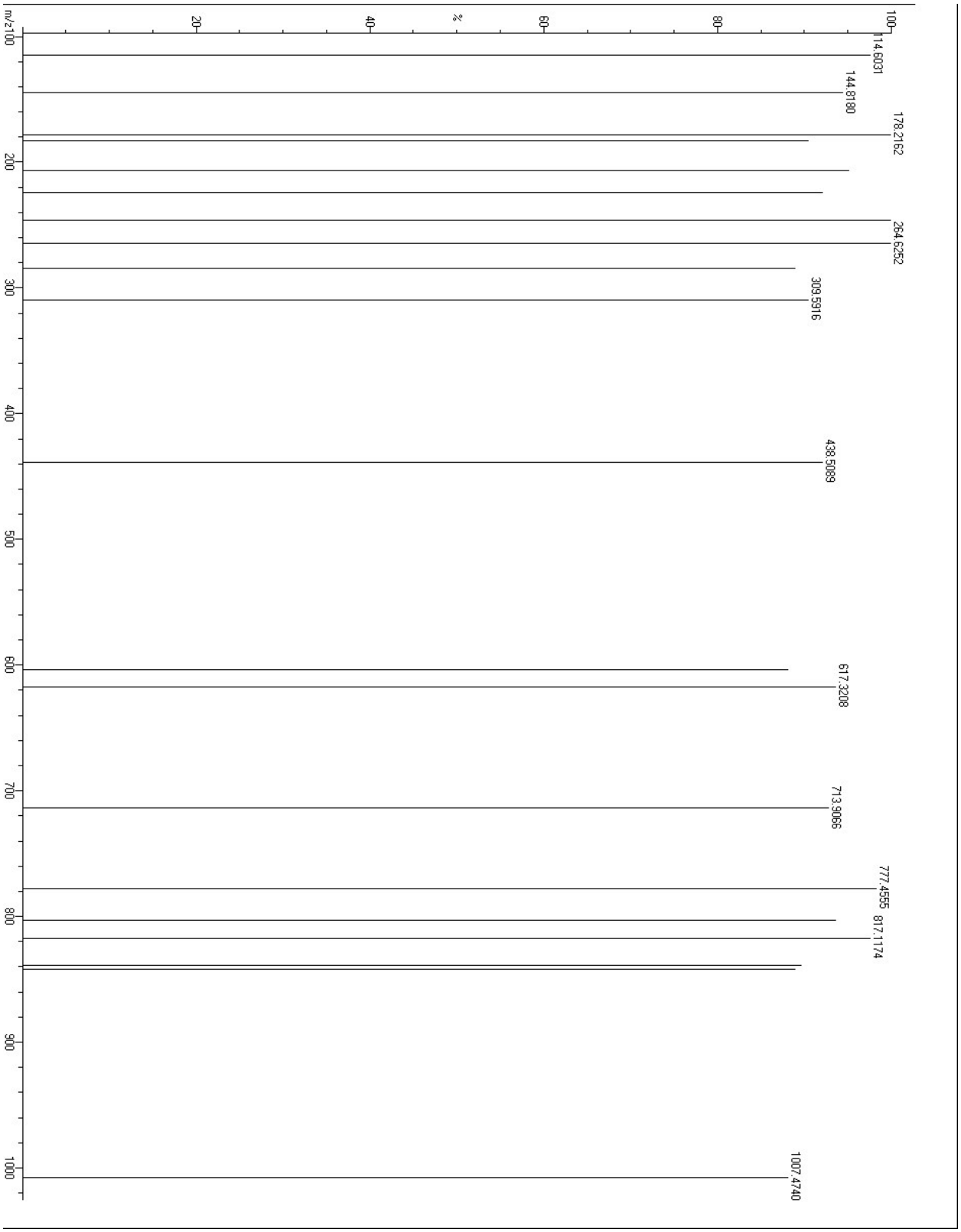


**Fig. S15** ESI-Mass spectrum of Compound **5**

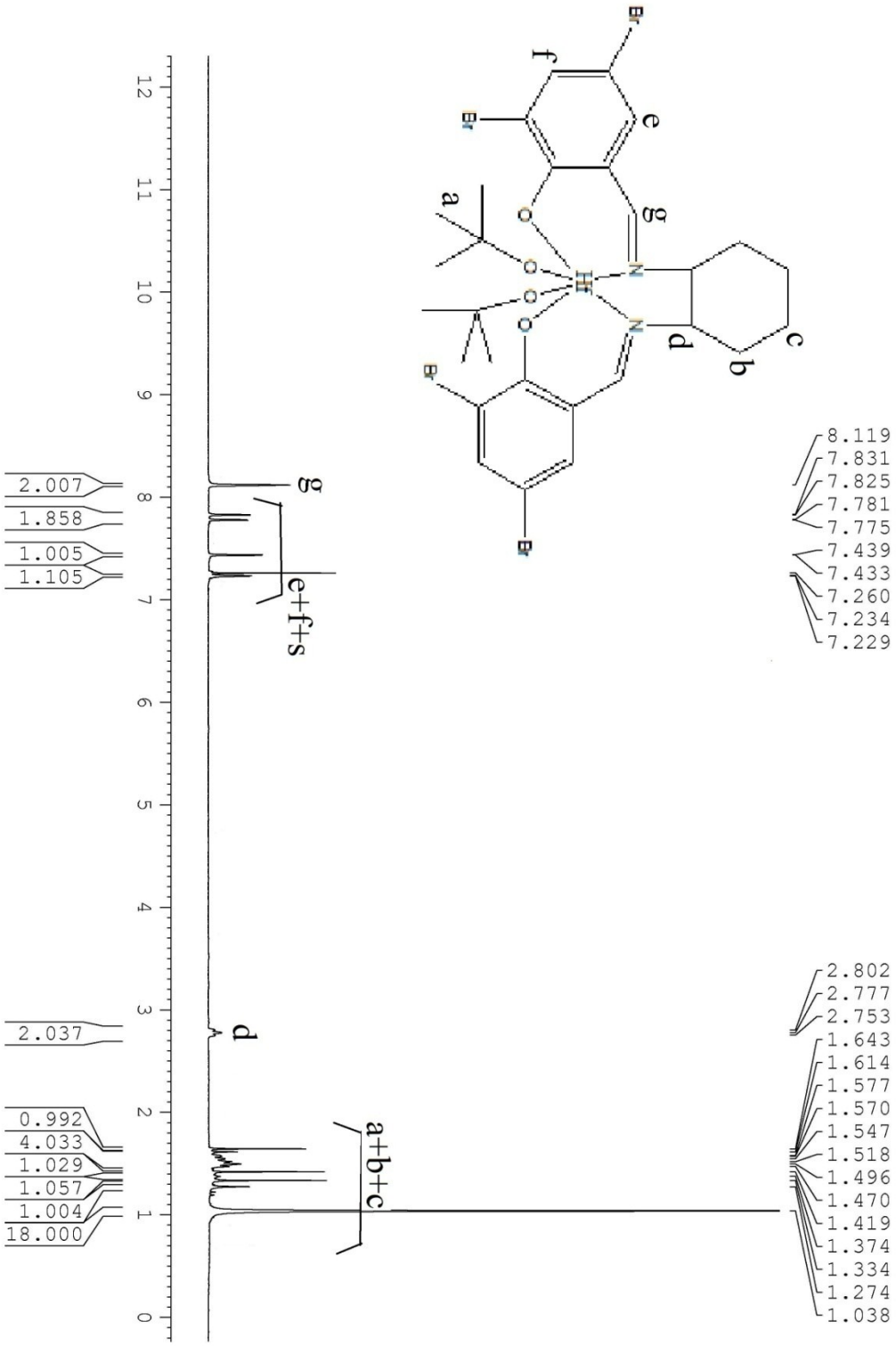


**Fig. S16** $^{1}$H NMR (400 MHz, $CDCl_3$) of Compound **6**

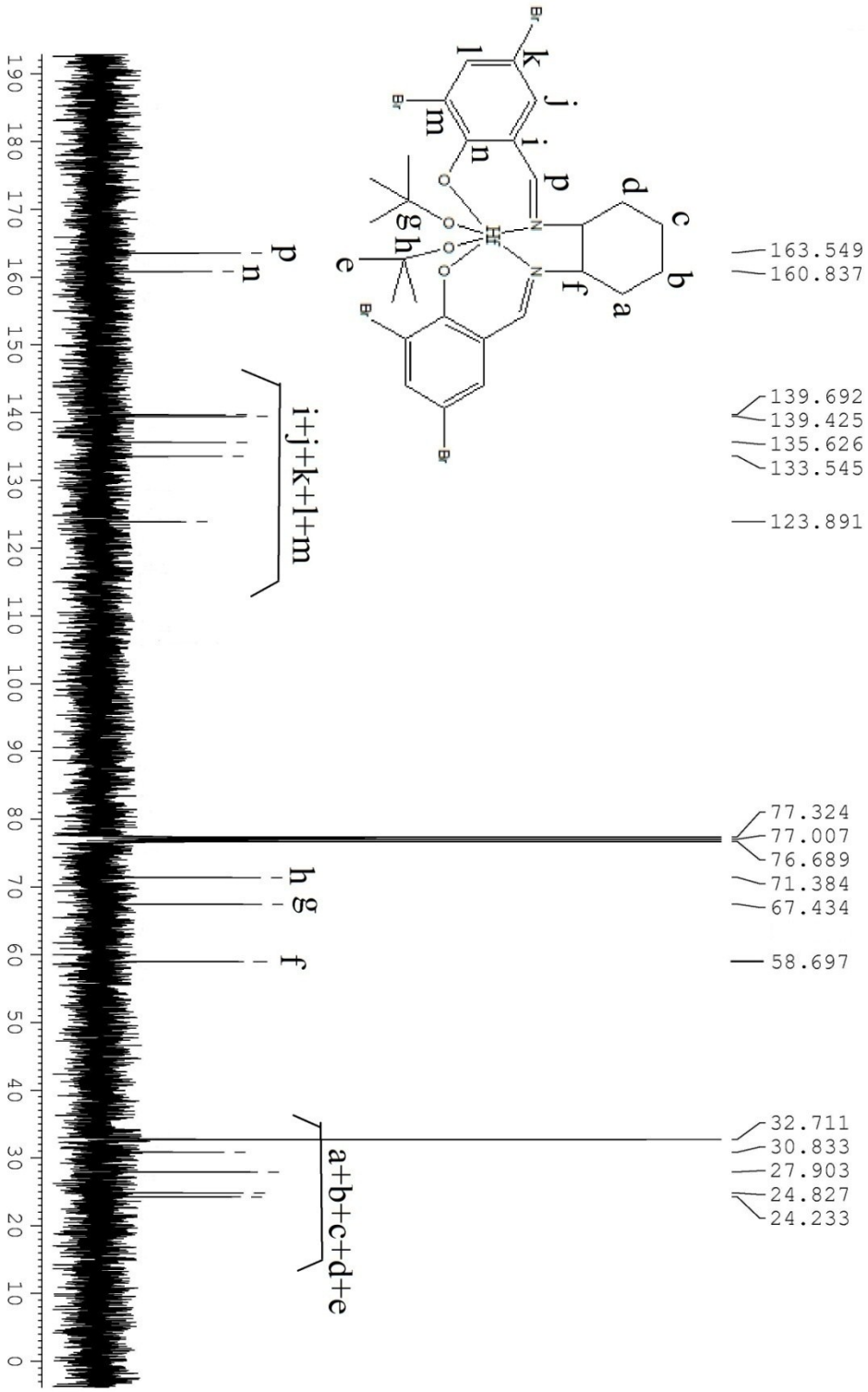


**Fig. S17** $^{13}C$ NMR (100 MHz, $CDCl_3$) of Compound **6**

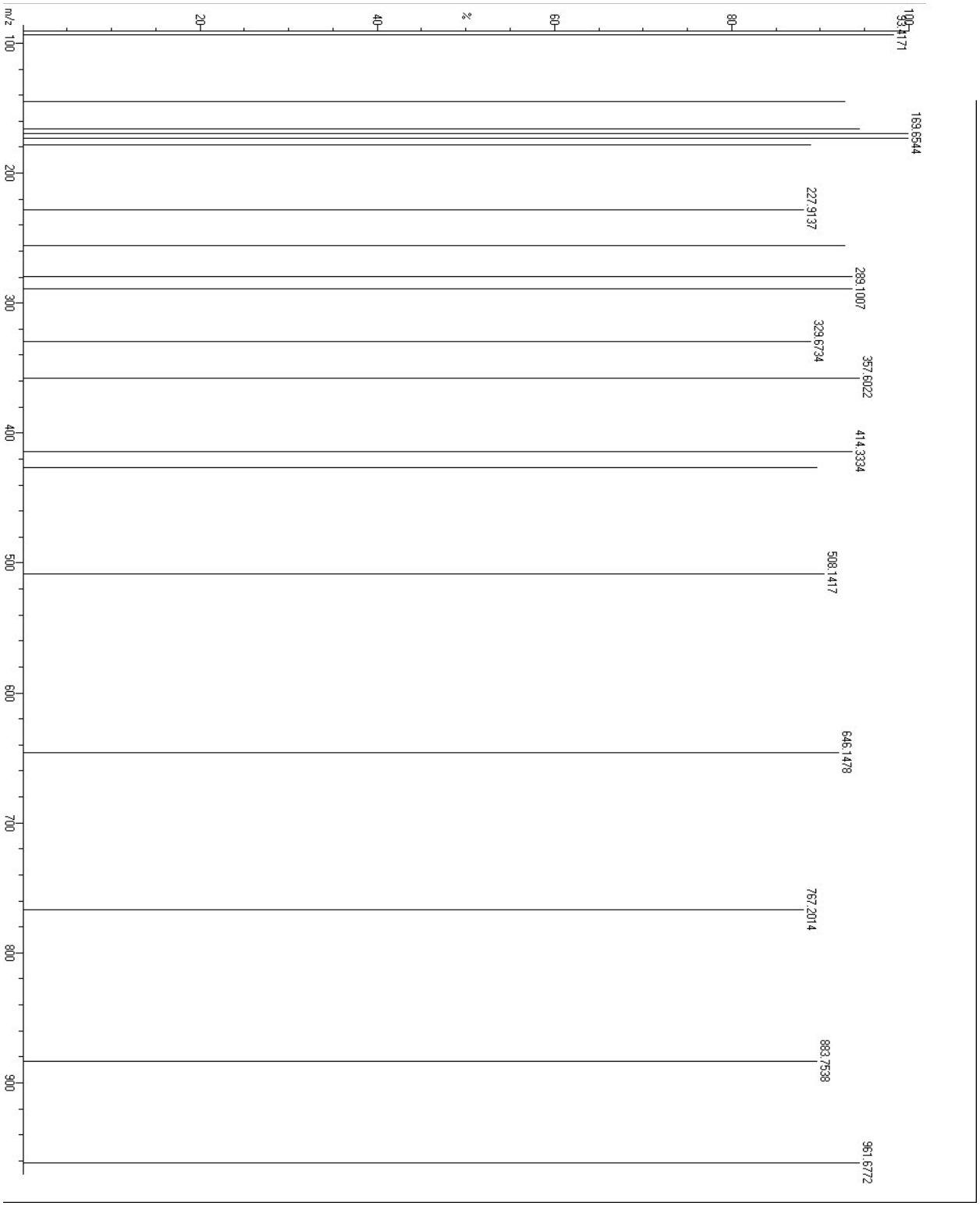


**Fig. S18** ESI-Mass spectrum of Compound **6**

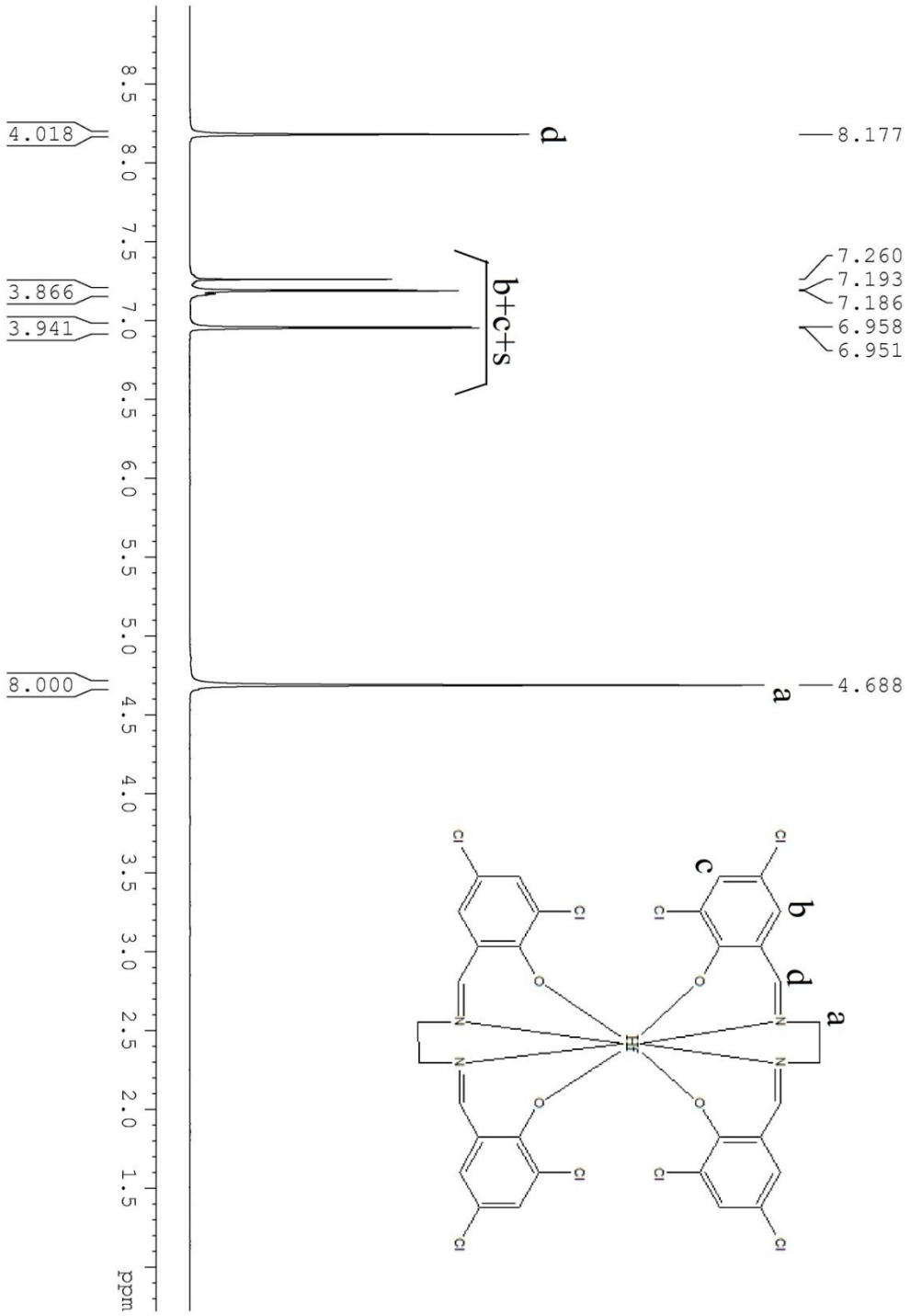


**Fig. S19** $^{1}$H NMR (400 MHz, $CDCl_3$) of Compound **7**

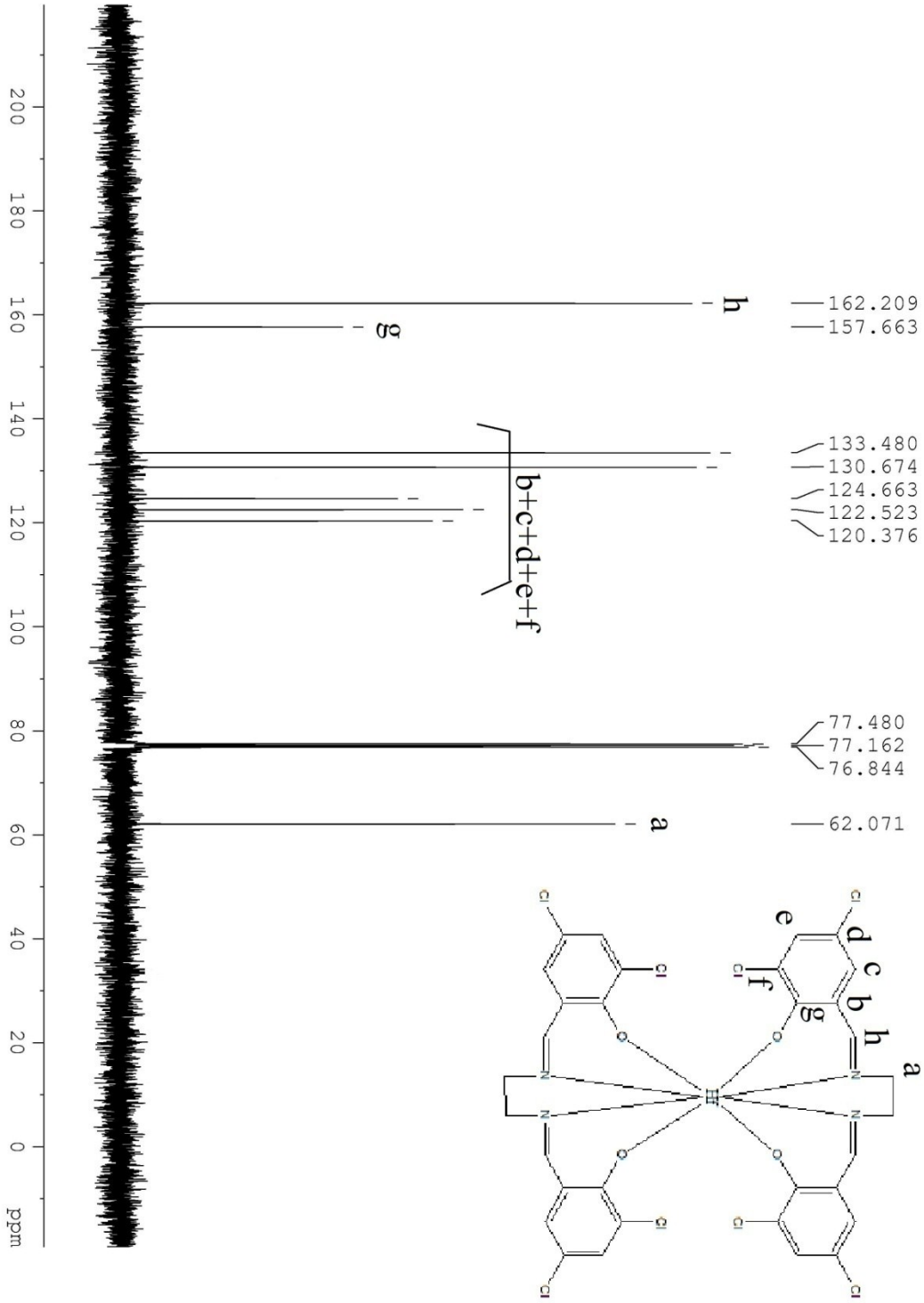


**Fig. S20** $^{13}C$ NMR (100 MHz, $CDCl_3$) of Compound **7**

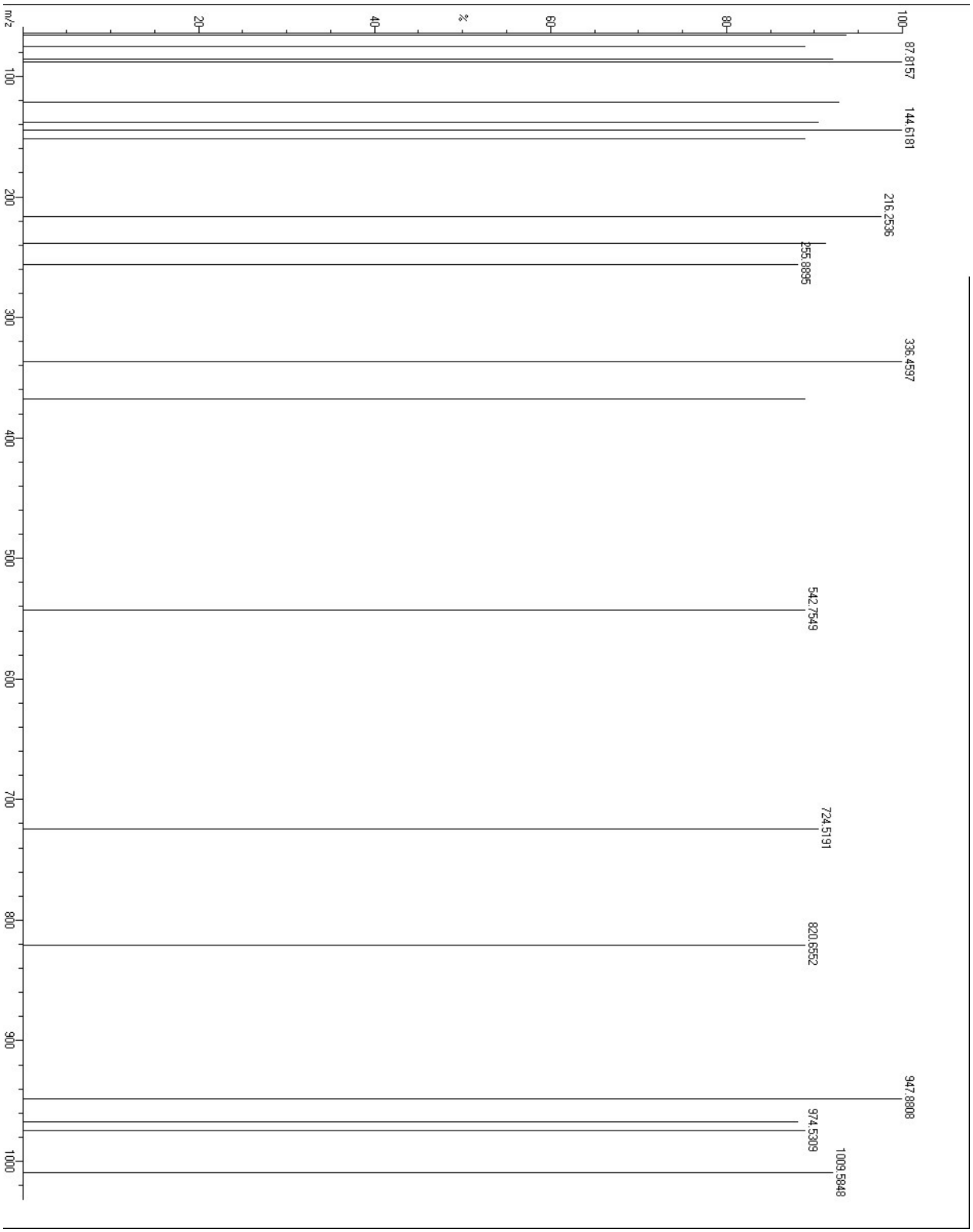


**Fig. S21** ESI-Mass Spectrum of Compound **7**

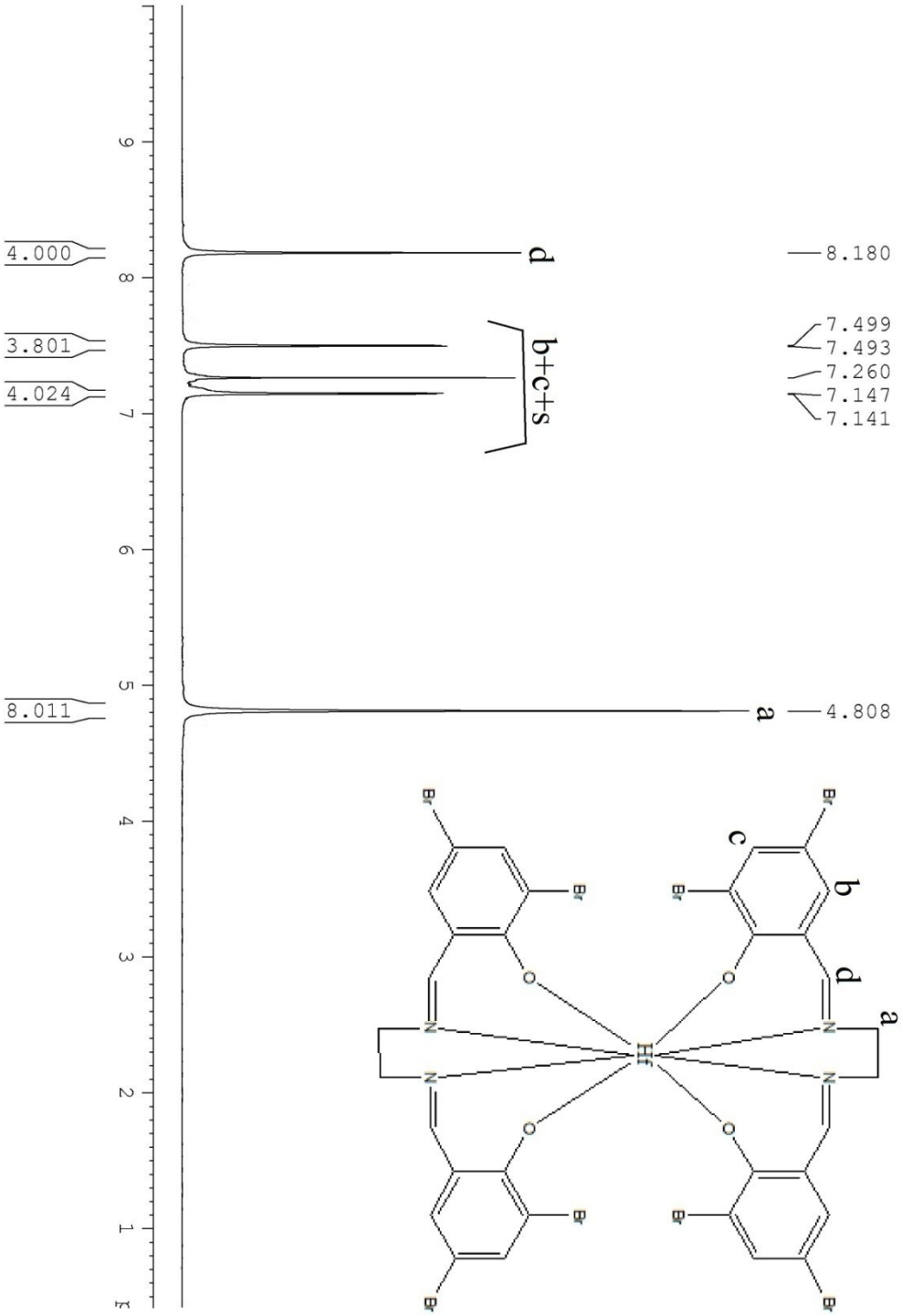


**Fig. S22** $^{1}$H NMR (400 MHz, $CDCl_3$) of Compound **8**

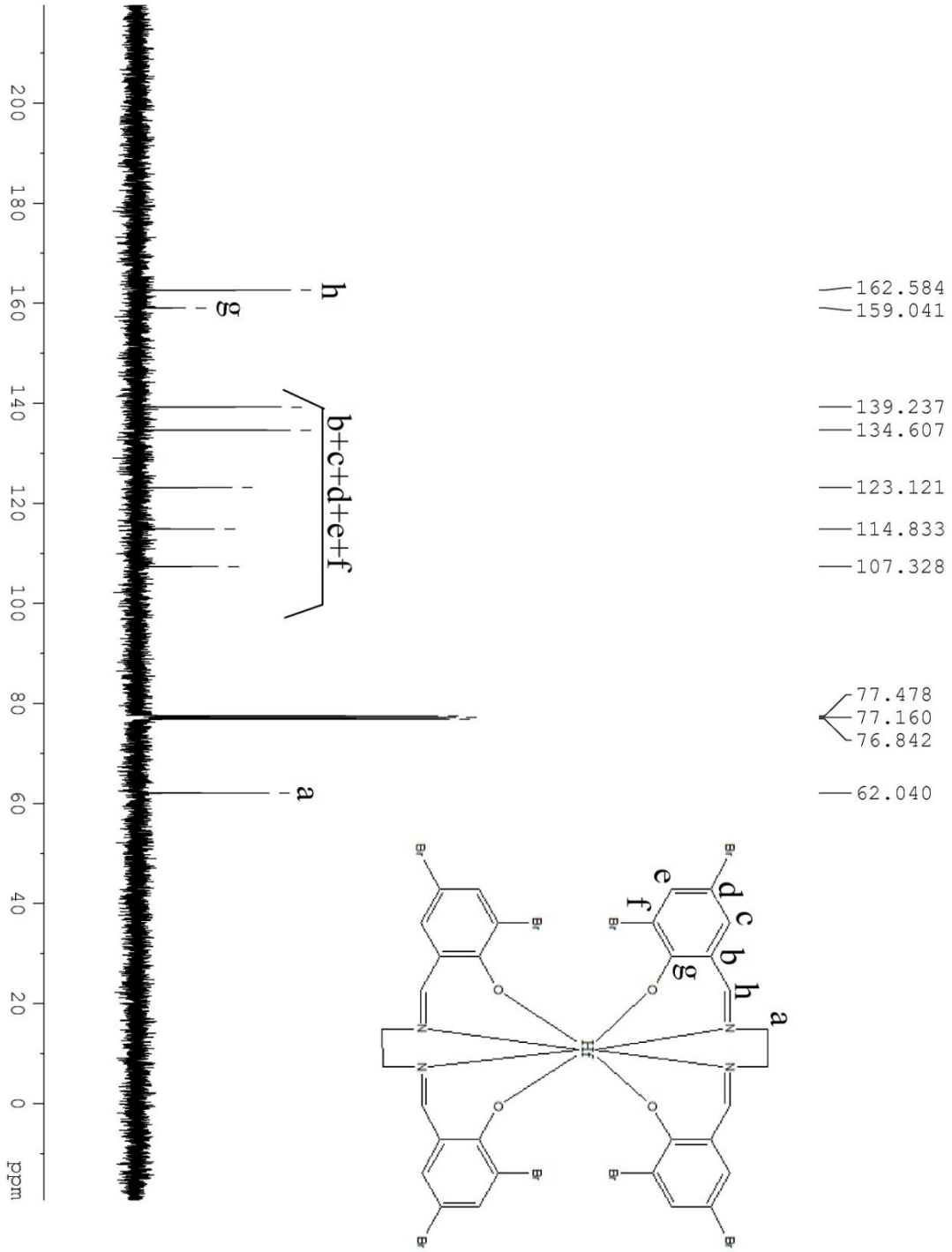


**Fig. S23** $^{13}C$ NMR (100 MHz, $CDCl_3$) of Compound **8**

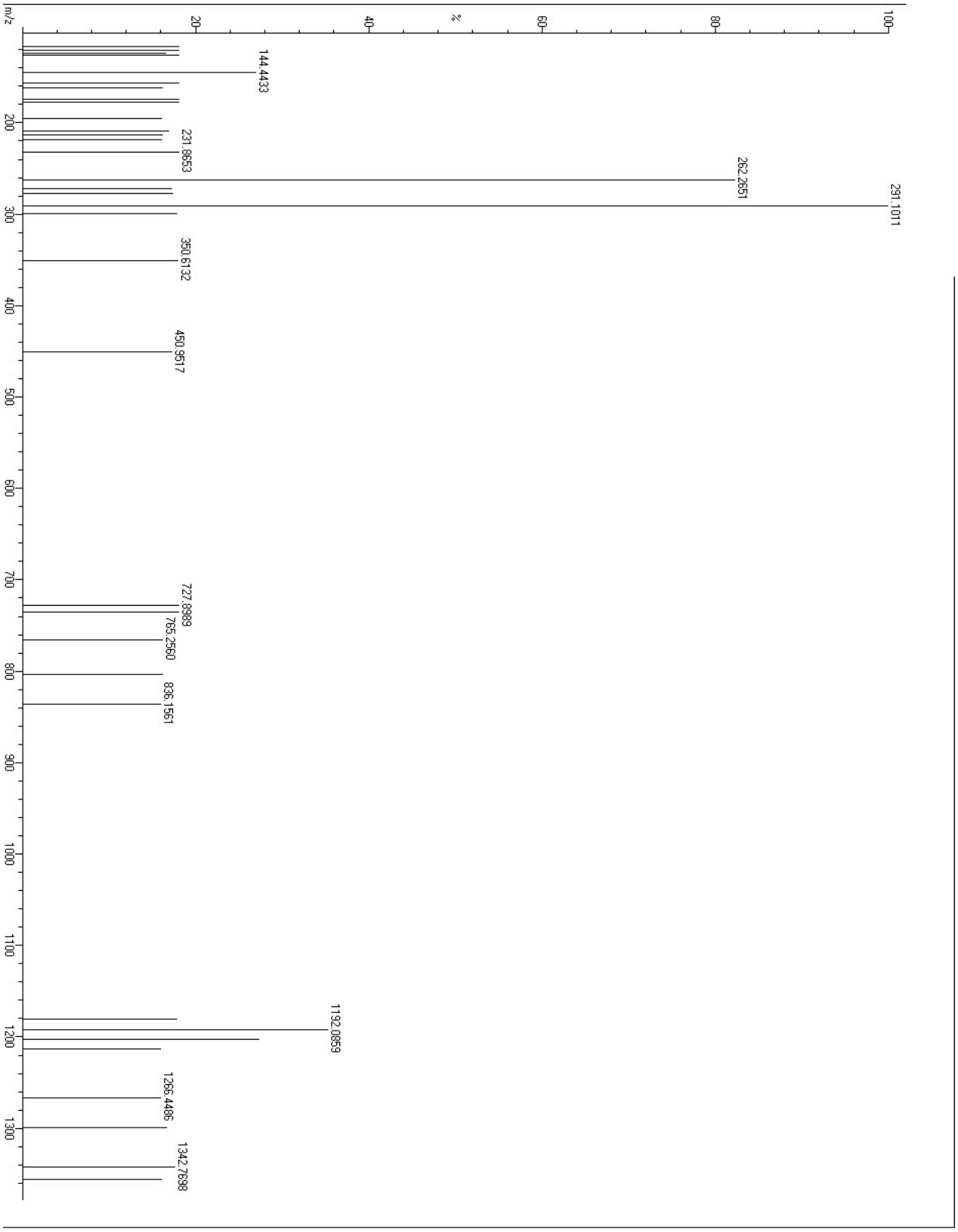


**Fig. S24** ESI-Mass Spectrum of Compound **8**

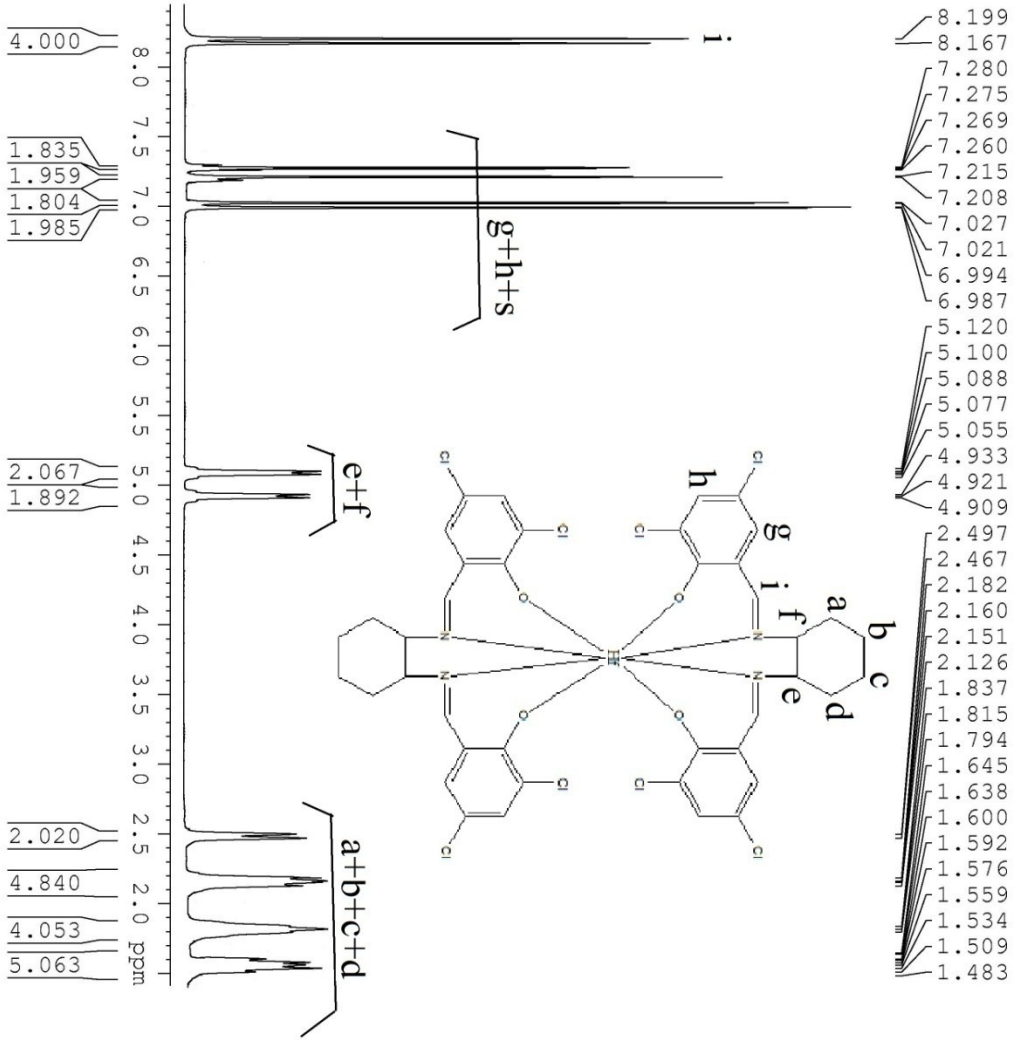


**Fig. S25** $^{1}$H NMR (400 MHz, $CDCl_3$) of Compound **9**

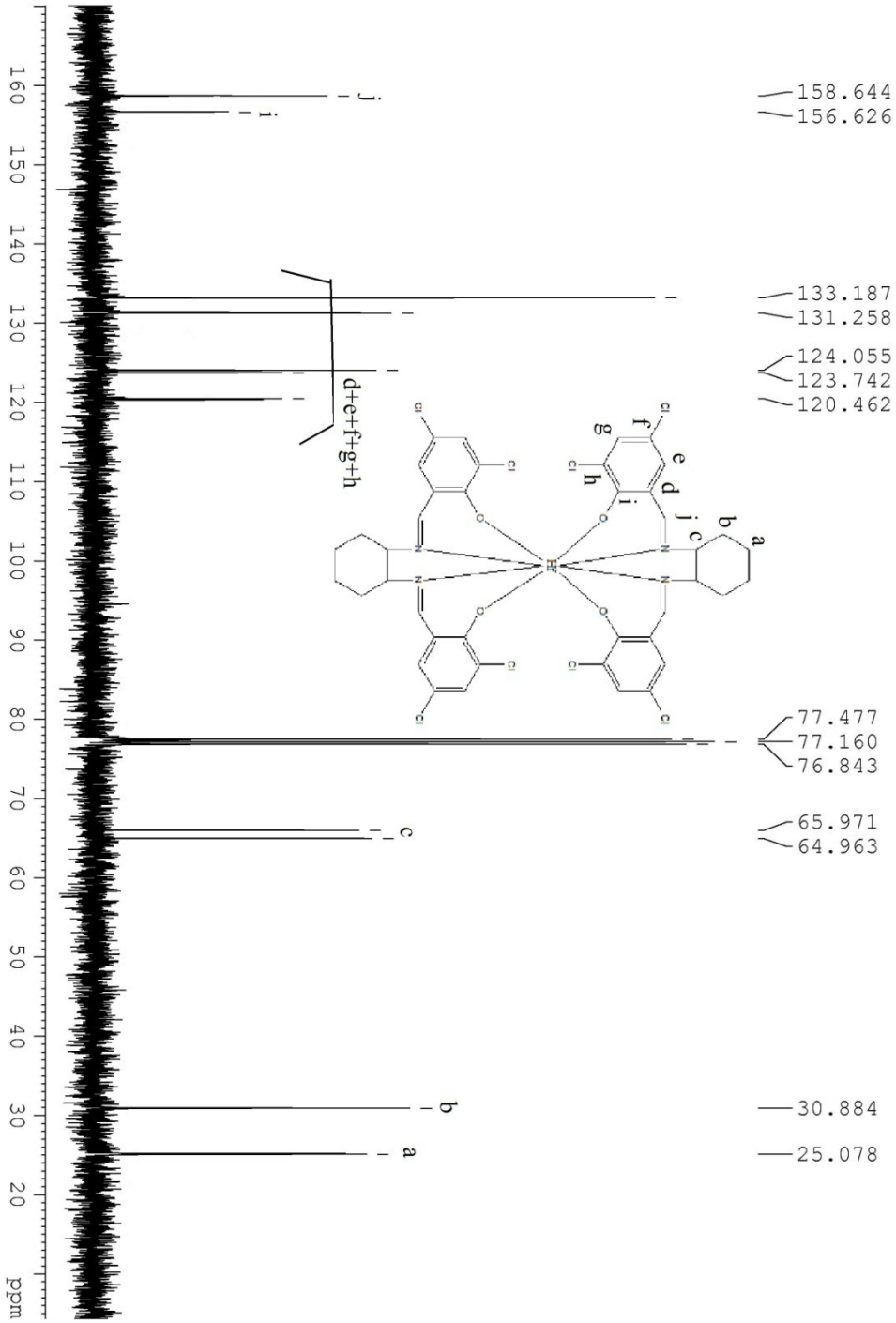


**Fig. S26** $^{13}C$ NMR (100 MHz, $CDCl_3$) of Compound **9**

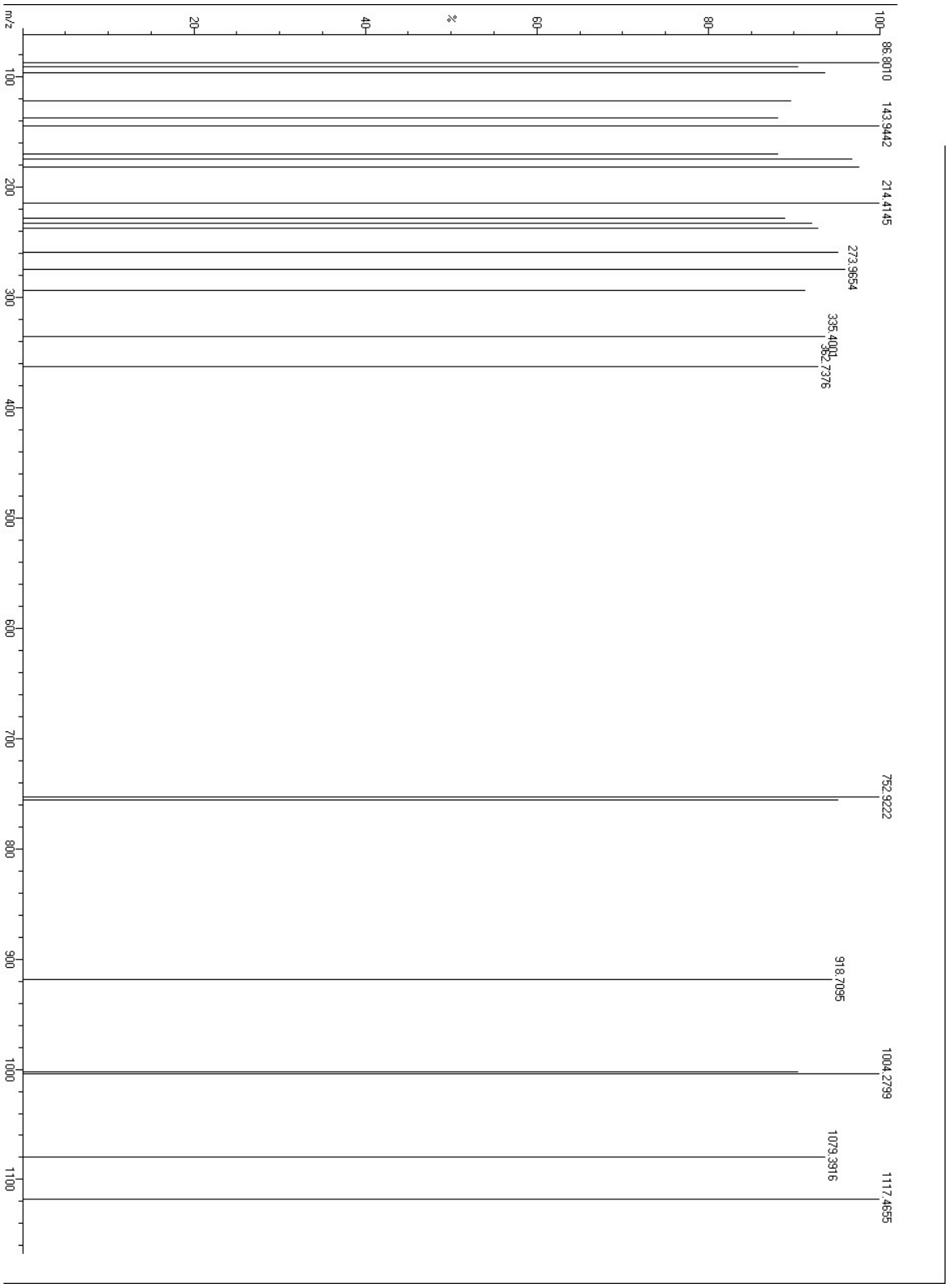


**Fig. S27** ESI-Mass Spectrum of Compound **9**

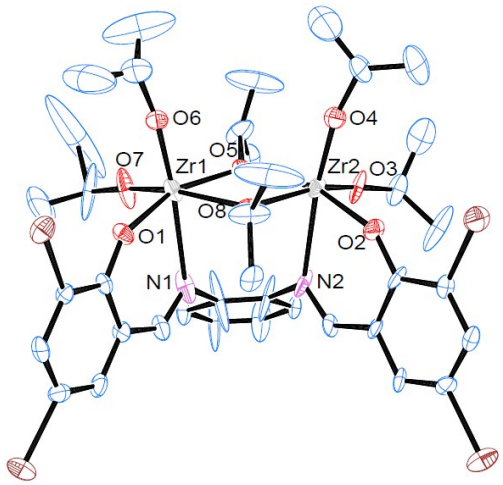


**Fig. S28** Molecular structure of **2**; thermal ellipsoids were drawn at 30 % probability level. Selected bond lengths (Å) and bond angles (°): Zr(1)-Zr(2) 3.496(2), Zr(1)-N(1) 2.479(15), Zr(2)-N(2) 2.472(13), Zr(1)-O(1) 2.062(9), Zr(1)-O(5) 2.143(9), Zr(2)-O(2) 2.050(8), Zr(2)-O(5) 2.161(8), O(4)-Zr(2)-Zr(1) 102.3(3), O(3)-Zr(2)-Zr(1) 127.8(3), O(2)-Zr(2)-Zr(1) 126.8(3), O(5)-Zr(2)-Zr(1) 35.5(2), N(2)-Zr(2)-Zr(1) 82.8(3), N(1)-Zr(1)-Zr(2) 83.7(3), O(6)-Zr(1)-Zr(2) 101.2(3), O(7)-Zr(1)-Zr(2) 126.7(3).

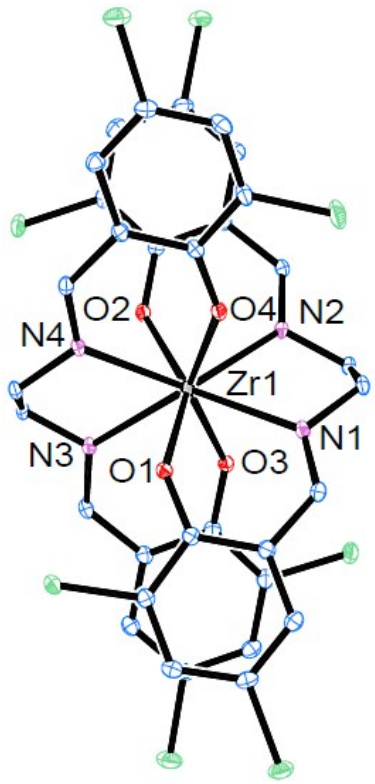


**Fig. S29** Molecular structure of **3**; thermal ellipsoids were drawn at 30 % probability level. Selected bond lengths (Å) and bond angles (°): N(1)-Zr(1) 2.4374(15), N(2)-Zr(1) 2.3928(14),

N(3)-Zr(1) 2.3960(14), N(4)-Zr(1) 2.4170(14), O(1)-Zr(1) 2.1011(12), O(2)-Zr(1) 2.1071(12), O(3)-Zr(1) 2.1082(12), O(4)-Zr(1) 2.0795(12), O(4)-Zr(1)-O(1) 95.61(5), O(4)-Zr(1)-O(3) 143.27(5), N(2)-Zr(1)-N(3) 129.73(5), N(3)-Zr(1)-N(4) 69.24(5).

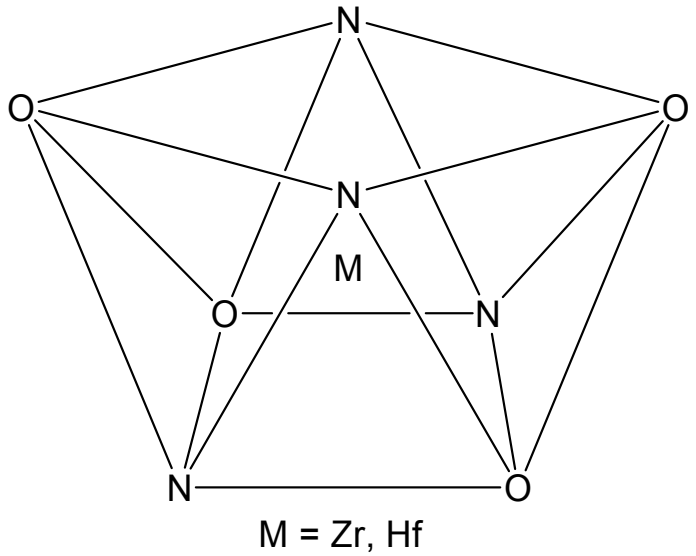


**Fig. S30** Coordination polyhedron of a distorted square antiprism geometry.

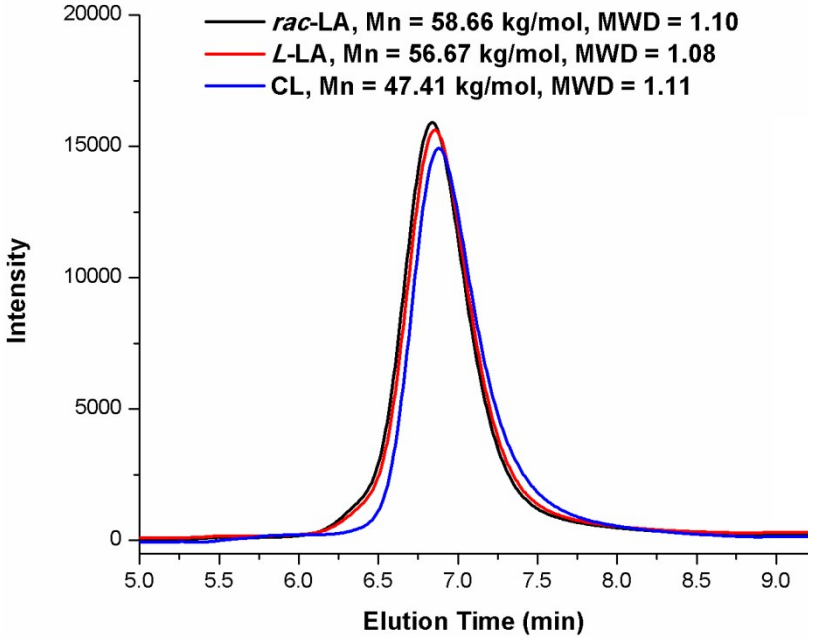


**Fig. S31** Representative GPC traces for the polymerization of (a) *rac*-LA (entry 2, Table 1); (b) *L*-LA (entry 11, Table 1) and (c) *ε*-CL (entry 14, Table 1) using **2**.

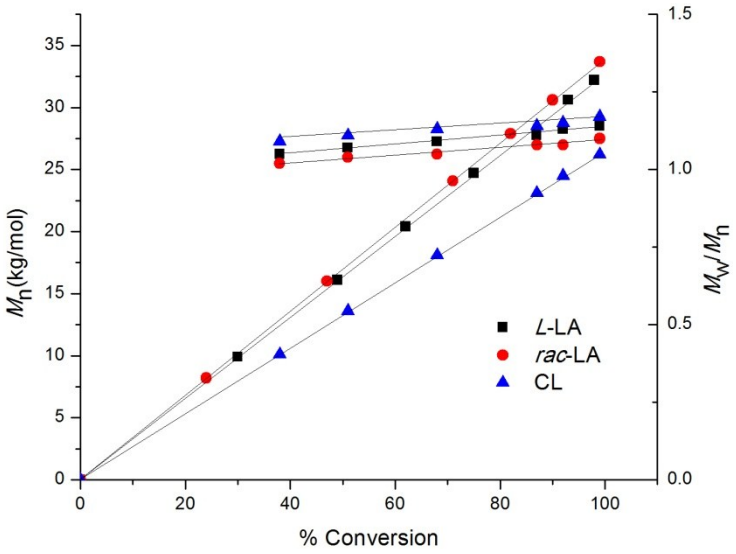


**Fig. S32** Plot of $M_n$ and $M_w/M_n$ vs. % conversion for *L*-LA, *rac*-LA and *ε*-CL polymerization using **2** at 140 °C (*L*-LA and *rac*-LA) and 80 °C (*ε*-CL).

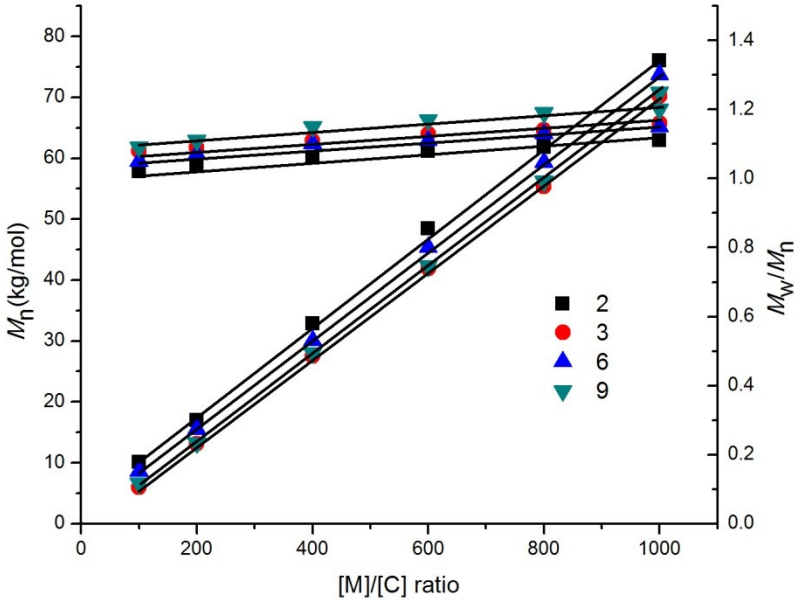


**Fig. S33** Plot of $M_n$ and $M_w/M_n$ *vs.* $[M]_0/[C]_0$ for *rac*-LA polymerization using **2**, **3**, **6** and **9** in the presence of benzyl alcohol at 140 °C.

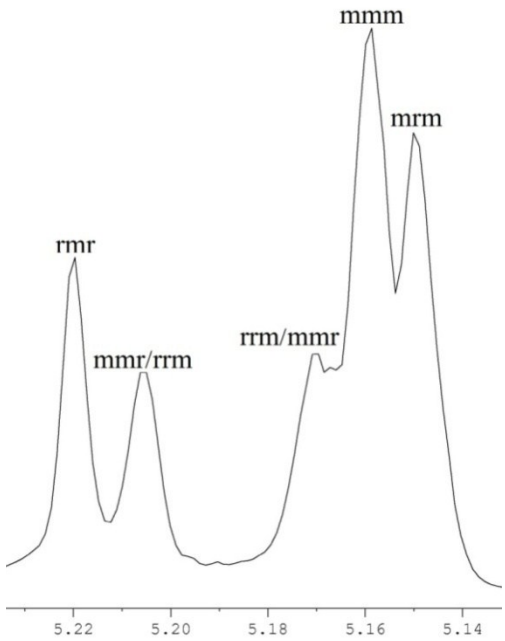


**Fig. S34** Homonuclear decoupled $^{1}$H NMR spectra of PLA from *rac*-LA using **2** in $CDCl_3$.

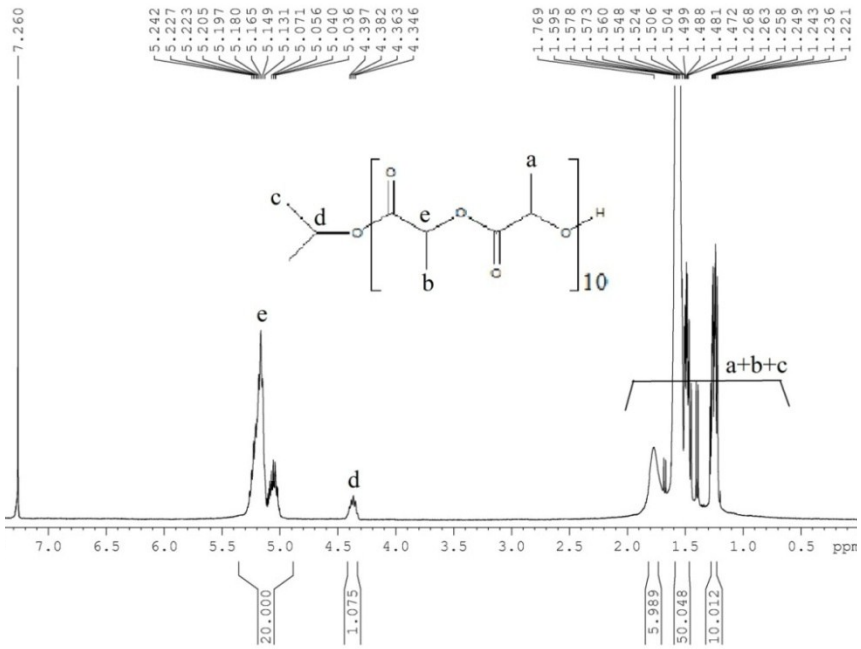


**Fig. S35** $^{1}$H NMR spectrum of the crude product obtained from a reaction between *rac*-LA and **2** in 15: 1 ratio.

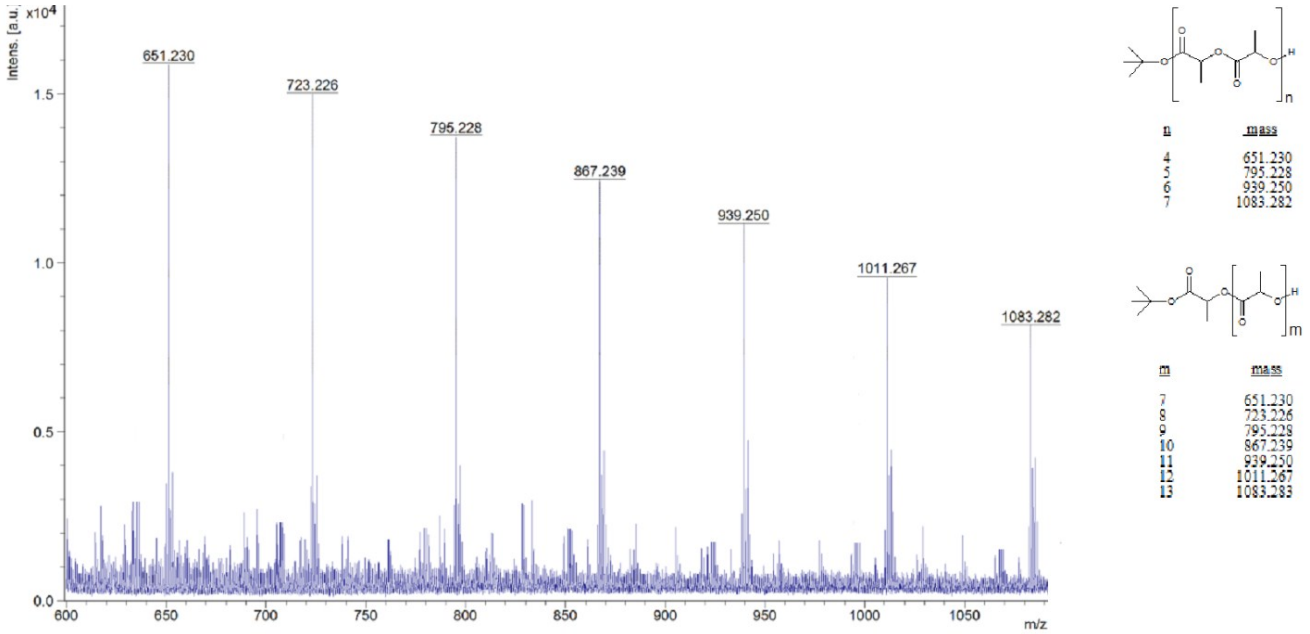


**Fig. S36** MALDI-TOF of the crude product obtained from a reaction between *rac*-LA and **6** in 10: 1 ratio.

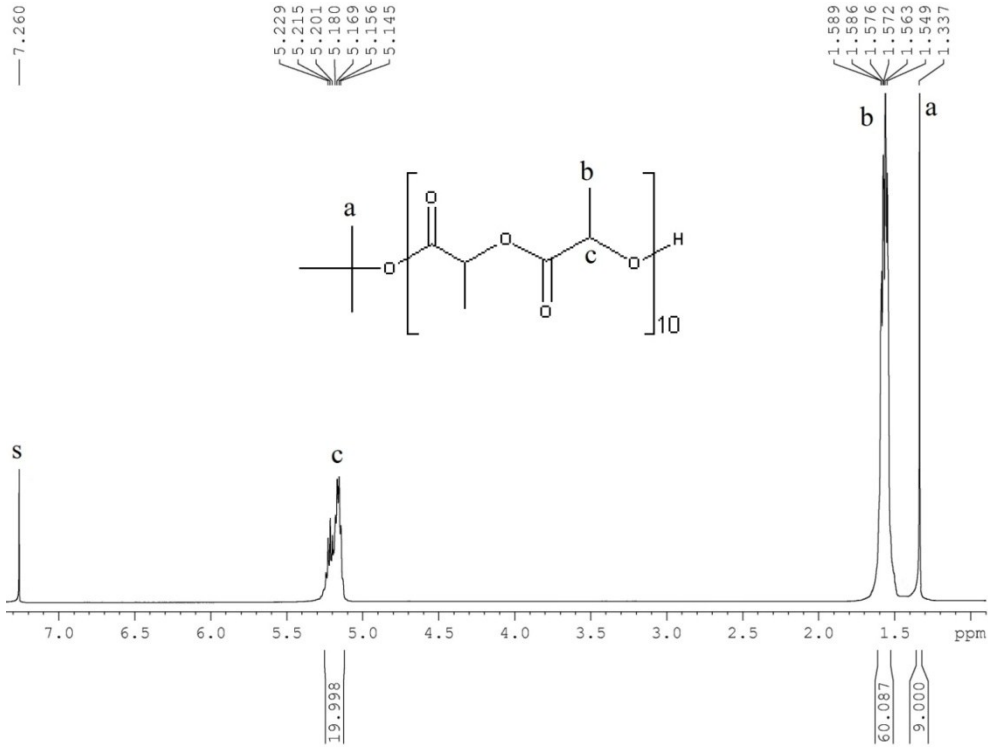


**Fig. S37** $^{1}$H NMR spectrum of the crude product obtained from a reaction between *rac*-LA and **6** in 10: 1 ratio.

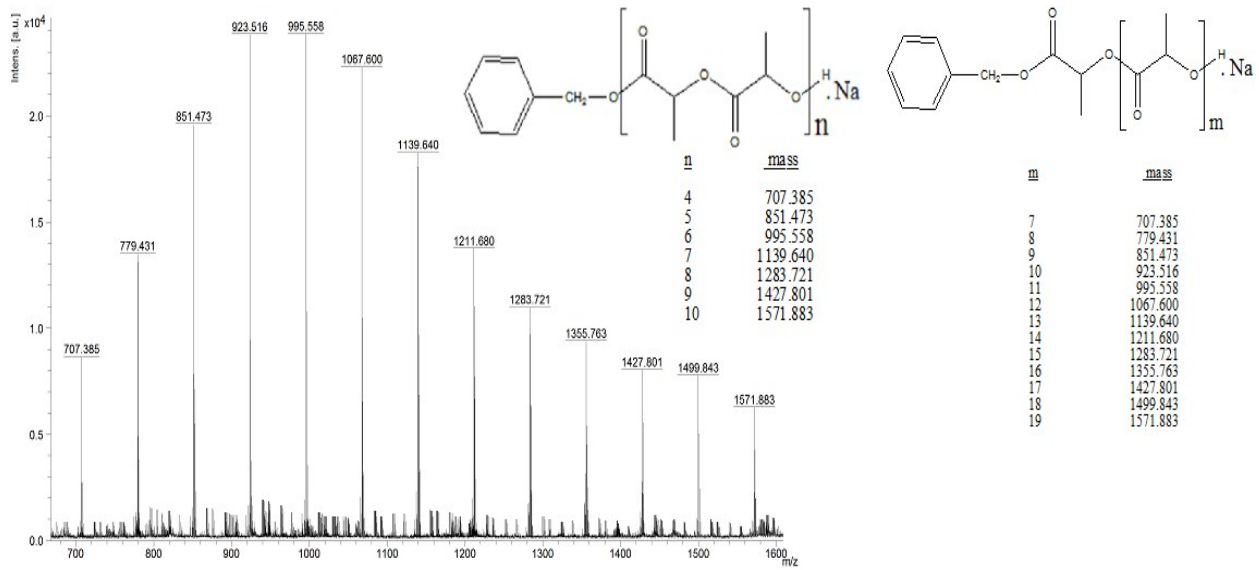


**Fig. S38** MALDI-TOF of the crude product obtained from a reaction between *rac*-LA and **2** in the presence of BnOH in 15: 1: 2 ratio.

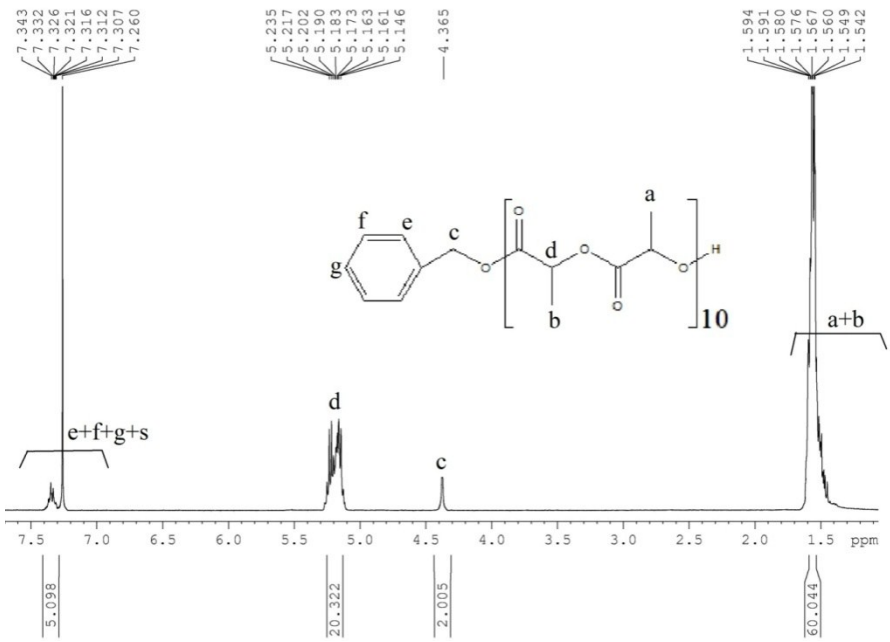


**Fig. S39** $^{1}$H NMR spectrum of the crude product obtained from a reaction between *rac*-LA and **2** in the presence of BnOH in ratio 15: 1: 2.

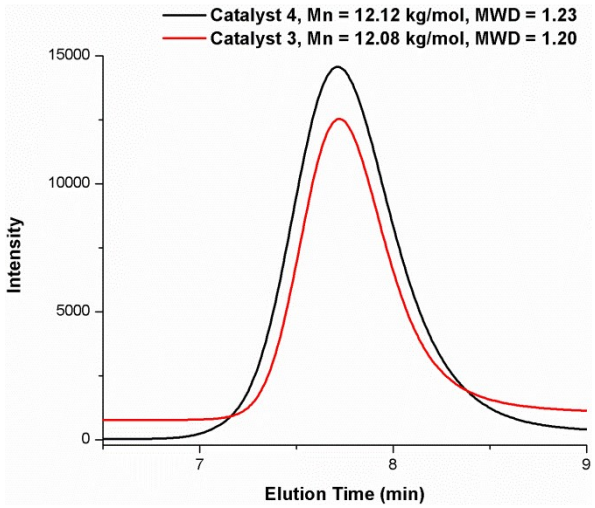


**Fig. S40** Representative GPC traces for the copolymerization of cyclohexene oxide and $CO_2$ using **3** (entry 6, Table 2) and **4** (entry 7, Table 2).

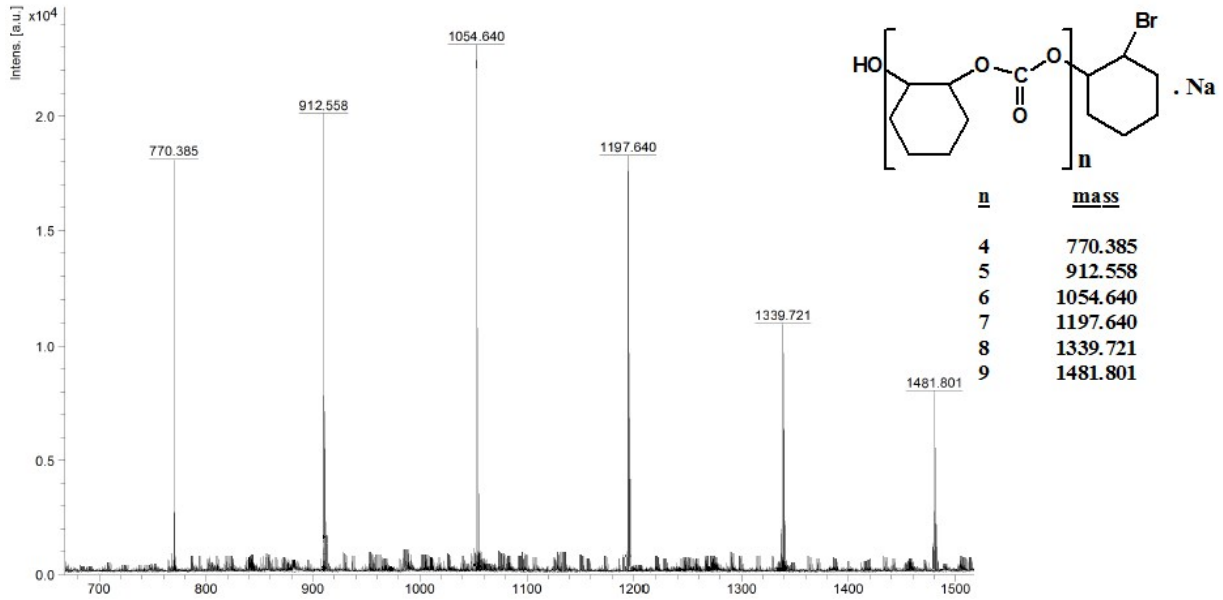


**Fig. S41** MALDI-TOF mass spectrum of PCHC sample produced by **2** at 50 °C and 35 bar $CO_2$ pressure from CHO and $CO_2$ using TBAB as cocatalyst.

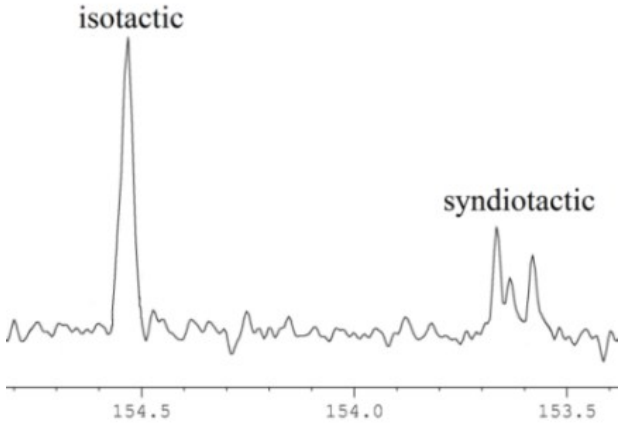


**Fig. S42** $^{13}C$ NMR spectrum of poly(cyclohexene carbonate) in the carbonate region produced from cyclohexene oxide and $CO_2$.

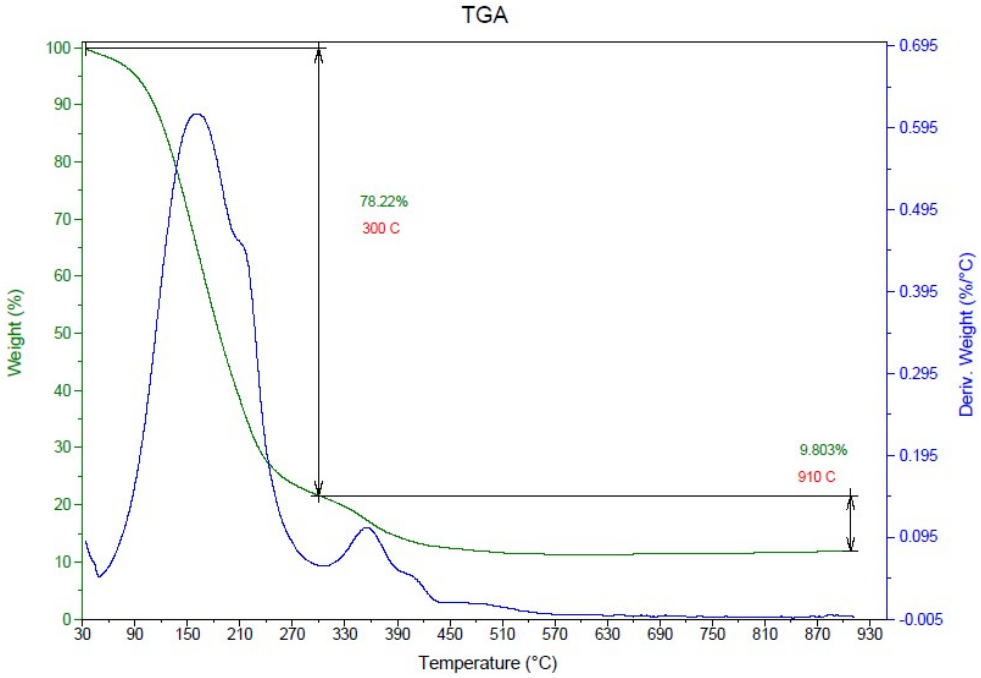


**Fig. S43** Representative TGA trace and derivative plot of PCHC produced by **2** (Table 2, entry 2).

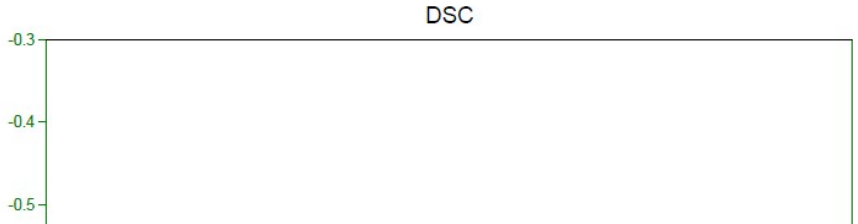

**Fig. S44** Representative DSC trace of PCHC produced by **2**, 2nd heat cycle (Table 2, entry 2).

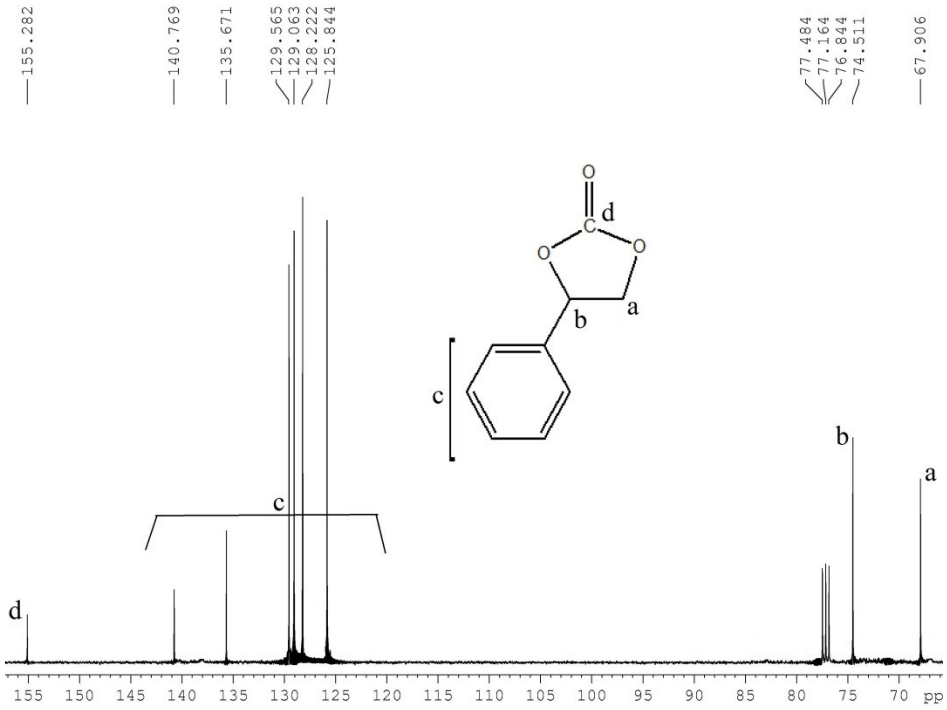


**Fig. S45** $^{13}C$ NMR spectrum of an aliquot from the reaction mixture of $SO/CO_2$ in $CDCl_3$.

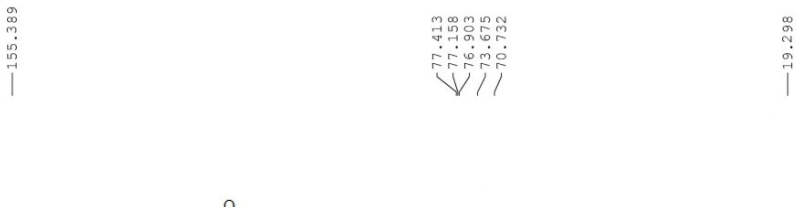

**Fig. S46** $^{13}C$ NMR spectrum of an aliquot from the reaction mixture of $PO/CO_2$ in $CDCl_3$.

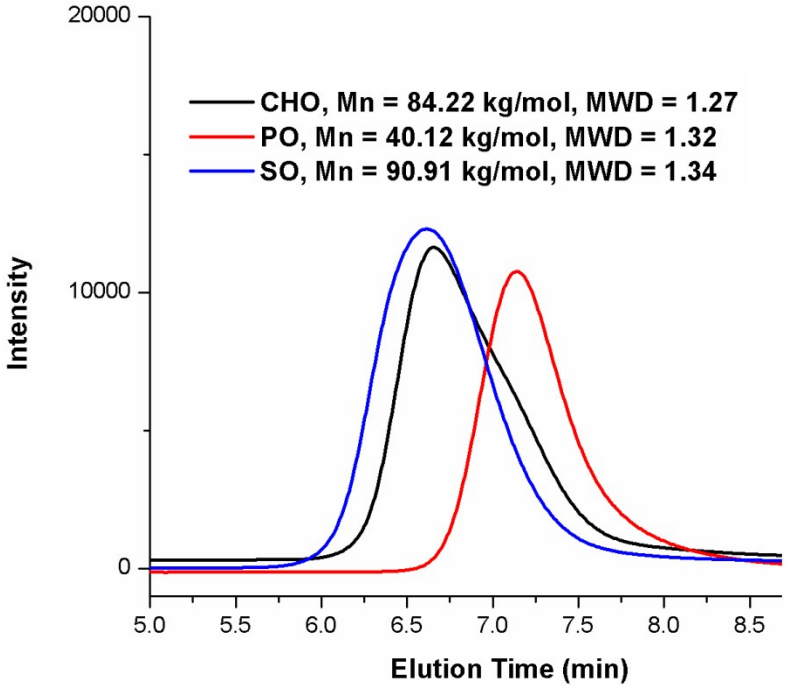


**Fig. S47** Representative GPC traces for the polymerization of (a) CHO (entry 3, Table 4); (b) PO (entry 12, Table 4) and (c) SO (entry 21, Table 4) using **3**.

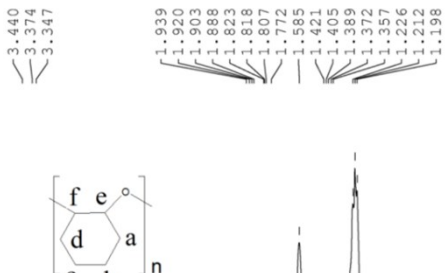

**Fig. S48** $^1$H NMR (500 MHz, $CDCl_3$) of the crude product obtained from a reaction between CHO and **2** in 1000: 1 ratio at 80 °C.

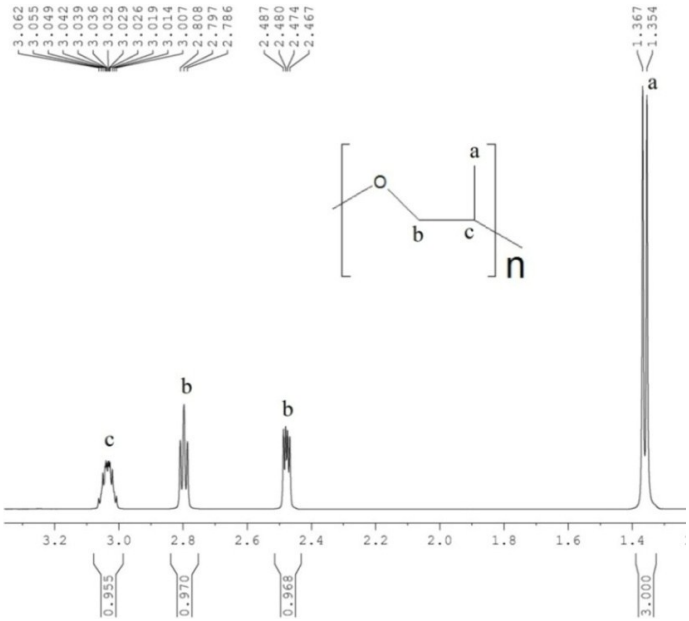


**Fig. S49** $^1$H NMR (500 MHz, $CDCl_3$) of the crude product obtained from a reaction between PO and **2** in 1000: 1 ratio at 40 °C.

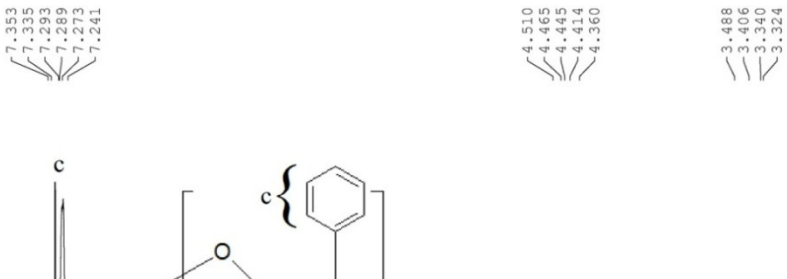

**Fig. S50** $^{1}$H NMR (500 MHz, $CDCl_3$) of the crude product obtained from a reaction between SO and **2** in 1000:1 ratio at 100 °C.

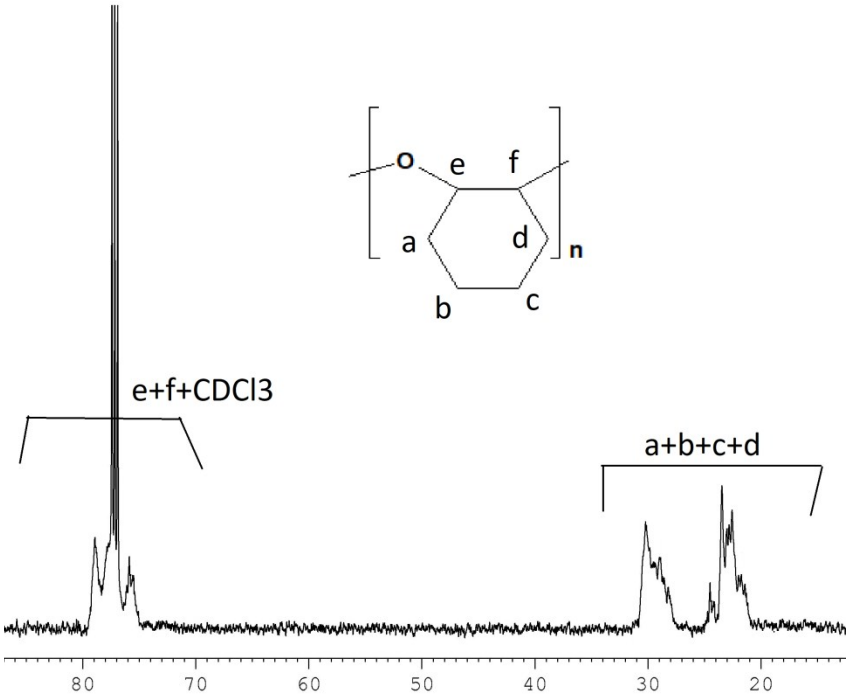


**Fig. S51** $^{13}$C NMR (125 MHz, $CDCl_3$) Spectrum of the representative PCHO obtained from a reaction between CHO and **2** in 1000: 1 ratio at 80 °C.

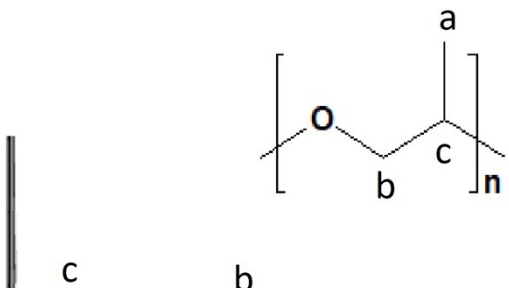

**Fig. S52** $^{13}C$ NMR (125 MHz, $CDCl_3$) Spectrum of the representative PPO obtained from a reaction between PO and **2** in 1000: 1 ratio at 40 °C.

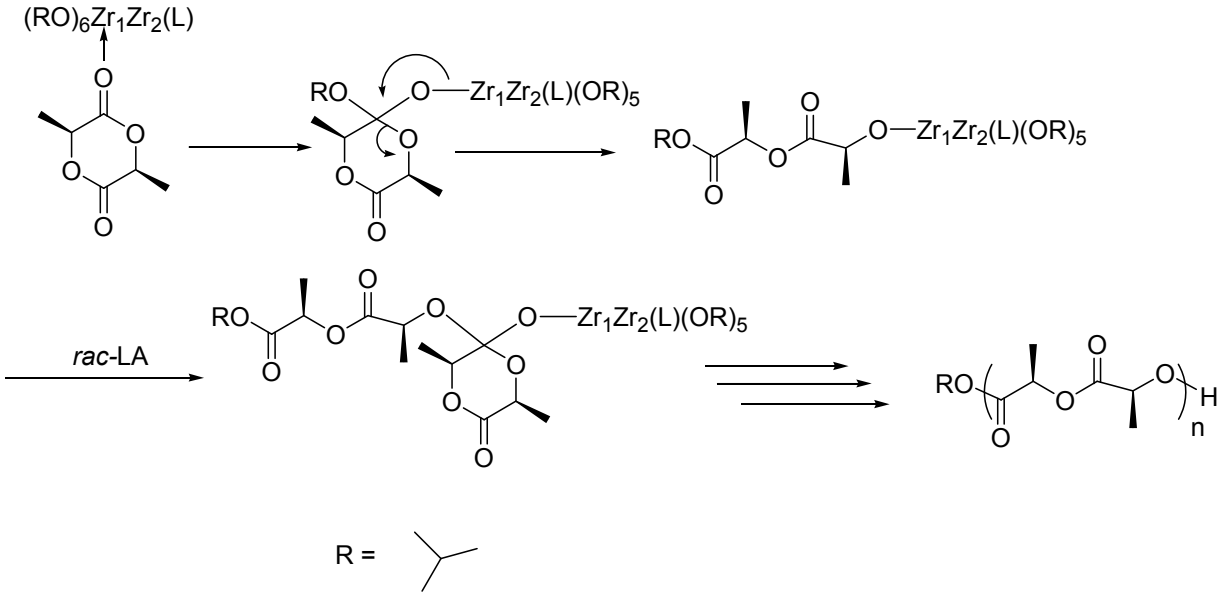


**Scheme S1** Polymerization proceeds through the coordination-insertion mechanism for *rac*-LA.

**Table S1** Crystal data for the structures of **1**, **2**, **3**, **5**, **6** and **9**

| Compounds | **1** | **2** | **3** | **5** | **6** | **9** |
|---|---|---|---|---|---|---|

| Emperical formula | $C_{50}H_{88}N_2O_8Zr_2$. $C_7H_8$ | $C_{38}H_{56}Br_4N_2O_8Zr_2$ | $C_{32}H_{20}Cl_8N_4O_4Zr$ | $C_{40}H_{28}Cl_8N_4O_4Zr$ | $C_{28}H_{32}Br_4HfN_2O_4$ | $C_{40}H_{32}Cl_8HfN_4O_4$ |
|---|---|---|---|---|---|---|
| Formula weight | 1119.80 | 1170.93 | 899.34 | 1003.48 | 958.69 | 1094.79 |
| Crystal system | Monoclinic | Monoclinic | Monoclinic | Orthorhombic | Monoclinic | Tetragonal |
| Space group | *P*2(1)/*n* | *P*2(1)/*n* | *P*2(1)/*c* | *Fdd*2 | *P*2(1)/*c* | *P*-42(1)*c* |
| Temp/K | 173(2) | 173(2) | 298(2) | 173(2) | 173(2) | 173(2) |
| Wavelength (Å) | 0.71073 | 0.71073 | 0.71073 | 0.71073 | 0.71073 | 0.71073 |
| *a* (Å) | 10.4865(3) | 10.3571(4) | 20.4732(6) | 26.427(3) | 11.9424(4) | 11.3471(2) |
| *b* (Å) | 30.3069(8) | 12.8862(6) | 12.5483(4) | 46.619(5) | 25.8050(10) | 11.3471(2) |
| *c* (Å) | 19.5427(5) | 35.6573(14) | 13.5794(4) | 12.8792(11) | 11.3456(3) | 16.1552(5) |
| $\alpha$ (°) | 90 | 90 | 90 | 90 | 90 | 90 |
| $\beta$ (°) | 101.0420(10) | 96.839(2) | 105.4610(10) | 90 | 111.2790(10) | 90 |
| $\gamma$ (°) | 90 | 90 | 90 | 90 | 90 | 90 |
| *V* (Å$^3$) | 6095.9(3) | 4725.1(3) | 3362.35(18) | 15867(3) | 3258.04(19) | 2080.09(8) |
| *Z* | 4 | 4 | 4 | 16 | 4 | 2 |
| $D_{calc}$ (g/cm$^3$) | 1.220 | 1.646 | 1.777 | 1.680 | 1.954 | 1.748 |
| Reflns collected | 41638 | 16563 | 24858 | 57581 | 27332 | 6745 |
| No. of indepreflns | 12814 | 5938 | 8358 | 13823 | 10150 | 2335 |
| GOF | 0.954 | 1.169 | 1.049 | 1.024 | 1.013 | 0.650 |
| F(000) | 2384 | 2328 | 1792 | 8064 | 1832 | 1080 |
| Final *R* indices($I$>2σ($I$)) | $R_1$ = 0.0344, $wR_2$ = 0.1127 | $R_1$ = 0.0830, $wR_2$ = 0.1658 | $R_1$ = 0.0255, $wR_2$ = 0.0558 | $R_1$ = 0.0455, $wR_2$ = 0.1010 | $R_1$ = 0.0379, $wR_2$ = 0.0663 | $R_1$ = 0.0218, $wR_2$ = 0.0713 |
| *R* indices (all data) | $R_1$ = 0.0457, $wR_2$ = 0.1255 | $R_1$ = 0.1106, $wR_2$ = 0.1752 | $R_1$ = 0.0356, $wR_2$ = 0.0608 | $R_1$ = 0.0691, $wR_2$ = 0.1134 | $R_1$ = 0.0720, $wR_2$ = 0.0747 | $R_1$ = 0.0301, $wR_2$ = 0.0835 |
| CCDC | 1815596 | 1422872 | 1815597 | 1815598 | 1815600 | 1815603 |

$R_1 = \sum|F_0| - |F_c|/\sum|F_0|$, $wR_2 = [\sum (F_0^2-F_c^2)^2/\sum w(F_0^2)^2]^{1/2}$

**Table S2** Polymerization data based on changing ratios in case of *rac*-LA using **1**, **2**, **3**, **5**, **6** and **9** in the presence of benzyl alcohol at 140 °C.

| Entry | Initiator | [M]/[C]/[BnOH] ratio | [a]Time/min | Yield (%) | [b]$M_n^{obs}$/ kgmol$^{-1}$ | [c]$M_n^{theo}$/ kgmol$^{-1}$ | $M_w/M_n$ |
|---|---|---|---|---|---|---|---|
| 1 | **1** | 100: 1: 2 | 28 | 95 | 9.52 | 6.95 | 1.04 |
| 2 | **1** | 200: 1: 2 | 60 | 94 | 17.0 | 13.6 | 1.07 |
| 3 | **1** | 400: 1: 2 | 101 | 99 | 31.4 | 28.6 | 1.09 |
| 4 | **1** | 600: 1: 2 | 149 | 98 | 46.0 | 42.5 | 1.10 |
| 5 | **1** | 800: 1: 2 | 202 | 99 | 61.1 | 57.2 | 1.12 |
| 6 | **1** | 1000: 1: 2 | 265 | 97 | 75.5 | 70.0 | 1.13 |
| 7 | **2** | 100: 1: 2 | 24 | 98 | 11.1 | 7.17 | 1.02 |
| 8 | **2** | 200: 1: 2 | 51 | 96 | 18.0 | 13.9 | 1.05 |
| 9 | **2** | 400: 1: 2 | 90 | 99 | 33.9 | 28.6 | 1.07 |
| 10 | **2** | 600: 1: 2 | 135 | 99 | 49.4 | 42.9 | 1.05 |
| 11 | **2** | 800: 1: 2 | 188 | 97 | 63.0 | 56.0 | 1.09 |
| 12 | **2** | 1000: 1: 2 | 248 | 96 | 77.0 | 69.3 | 1.11 |
| 13 | **3** | 100: 1: 2 | 39 | 95 | 7.01 | 6.95 | 1.08 |
| 14 | **3** | 200: 1: 2 | 85 | 94 | 14.1 | 13.6 | 1.09 |

| | | | | | | | |
|---|---|---|---|---|---|---|---|
| 15 | **3** | 400: 1: 2 | 127 | 99 | 28.5 | 28.6 | 1.13 |
| 16 | **3** | 600: 1: 2 | 179 | 98 | 42.9 | 42.5 | 1.11 |
| 17 | **3** | 800: 1: 2 | 242 | 99 | 56.4 | 57.2 | 1.14 |
| 18 | **3** | 1000: 1: 2 | 305 | 97 | 71.2 | 70.0 | 1.16 |
| 19 | **5** | 100: 1: 2 | 34 | 98 | 8.01 | 7.17 | 1.06 |
| 20 | **5** | 200: 1: 2 | 70 | 99 | 15.0 | 14.4 | 1.08 |
| 21 | **5** | 400: 1: 2 | 112 | 95 | 29.2 | 27.5 | 1.10 |
| 22 | **5** | 600: 1: 2 | 163 | 94 | 43.9 | 40.7 | 1.09 |
| 23 | **5** | 800: 1: 2 | 220 | 99 | 57.8 | 57.2 | 1.12 |
| 24 | **5** | 1000: 1: 2 | 285 | 98 | 72.8 | 70.7 | 1.14 |
| 25 | **6** | 100: 1: 2 | 31 | 99 | 9.6 | 7.25 | 1.05 |
| 26 | **6** | 200: 1: 2 | 64 | 97 | 16.5 | 14.1 | 1.07 |
| 27 | **6** | 400: 1: 2 | 106 | 95 | 31.0 | 27.5 | 1.10 |
| 28 | **6** | 600: 1: 2 | 155 | 98 | 46.4 | 42.5 | 1.11 |
| 29 | **6** | 800: 1: 2 | 209 | 96 | 60.3 | 55.4 | 1.13 |
| 30 | **6** | 1000: 1: 2 | 270 | 95 | 74.7 | 68.6 | 1.15 |
| 31 | **9** | 100: 1: 2 | 37 | 97 | 7.66 | 7.10 | 1.09 |
| 32 | **9** | 200: 1: 2 | 79 | 97 | 14.3 | 14.1 | 1.11 |
| 33 | **9** | 400: 1: 2 | 124 | 94 | 29.0 | 27.2 | 1.15 |
| 34 | **9** | 600: 1: 2 | 171 | 95 | 43.3 | 41.2 | 1.17 |
| 35 | **9** | 800: 1: 2 | 235 | 98 | 57.2 | 56.6 | 1.19 |
| 36 | **9** | 1000: 1: 2 | 297 | 95 | 72.3 | 68.6 | 1.20 |

[a]Time of polymerization measured by quenching the polymerization reaction when all monomer was found consumed. [b]Measured by GPC at 27 °C in THF relative to polystyrene standards after applying a multiplication factor of 0.58 (for *rac*-LA). [c]$M_n$ (theoretical) at actual conversion = [Conversion × $[M]_0/[C]_0$ × mol. Wt. (monomer)] + mol. Wt. (BnOH).

**Table S3** DSC and TGA measurements for the different copolymers obtained in **Table 2**.

| Entry | Initiator | Copolymers | $T_g$[a] (°C) | $T_{d5}$[b] (°C) | $T_{d50}$[b] (°C) | $T_{d95}$[b] (°C) |
|---|---|---|---|---|---|---|
| 1 | **2** | PCHC | 55 | 92 | 187 | >900 |
| 2 | **3** | PCHC | 48 | 85 | 179 | >900 |
| 3 | **6** | PCHC | 52 | 90 | 185 | >900 |
| 4 | **9** | PCHC | 50 | 88 | 182 | >900 |

[a]$T_g$ values represent the midpoint temperature during the second heating cycle determined by DSC. [b]$T_{d5}$, $T_{d50}$, and $T_{d95}$ are the decomposition temperature at 5%, 50%, and 95% weight loss, respectively determined by TGA analysis.